7-2021

Soil Morphology and Carbon Stocks of Deflation Basin Wetlands in Eastern Nebraska, USA

Aubrey Grace Kemper
University of Nebraska-Lincoln, aubrey.kemper@huskers.unl.edu

Soil Morphology and Carbon Stocks of Deflation Basin Wetlands in Eastern Nebraska, USA

by

Aubrey Grace Kemper

A THESIS

Presented to the Faculty of

The Graduate College at the University of Nebraska

In Partial Fulfillment of Requirements

For the Degree of Master of Science

Major: Natural Resource Sciences

Under the Supervision of Professor Judith K. Turk

Lincoln, Nebraska

July 2021

SOIL MORPHOLOGY AND CARBON STOCKS OF DEFLATION BASIN WETLANDS IN EASTERN NEBRASKA, USA

Aubrey Grace Kemper, M.S.

University of Nebraska, 2021

Advisor: Judith K. Turk

Wetlands contribute important ecosystem services such as water filtration and storage, wildlife habitat, and carbon sequestration. The objective of this study is to compare the soil morphology and the carbon and nitrogen stocks between the upland, basin edge, and basin floor in playa wetlands of eastern Nebraska. This work was conducted in three deflation basin wetlands in the Todd Valley, a loess-mantled, former course of the Platte River, in eastern Nebraska. Soil morphological descriptions were evaluated to two meters' depth using cores collected along three transects from the upland to the basin floor in three basins, carbon and nitrogen stocks were evaluated for each core, and particle size analysis determined for a subset of the cores. Results show evidence of colluviation, leaching and accumulation of pedogenic clay, and the presence of diffuse carbonates in one basin. Comparisons of carbon and nitrogen stocks between the basins and uplands showed varied trends between the three basins. One basin had the highest carbon and nitrogen stock in the uplands, another had the highest carbon and nitrogen stocks on the basin floor (due to a buried soil in the profile), and another showed no significant difference in carbon and nitrogen stocks in relation to transect position. Profile distributions of carbon suggest that the limited carbon storage in these wetlands is, at least in part, due to leaching losses of dissolved organic carbon. Future efforts toward wetland restoration in eastern Nebraska should

consider what the soil morphology and characterization data indicate about the legacy of basin infilling, as well as carbon sequestration of these distinctive wetlands.

DEDICATION

I dedicate this thesis to the blessed memory of my grandfather, Mr. Albert Kohnke. May his memory be for a blessing on his grandchildren and great-grandchildren, who never knew him in life but have always felt his love through those in our lives who did.

ACKNOWLEDGEMENTS

I would like to acknowledge the help of the following people who have helped me get to where I am today:

- My parents, Patty and Bob Kemper, for being my first and greatest advocates and investing time and money to ensure I received the best education possible.
- My family – biological and chosen – who loved me unconditionally and encouraged me every step of the way.
- My schoolteachers, who saw potential in me and pushed me to be my best.
- Everyone in the Department of Natural Sciences at Flagler College, who got to know me as a person and worked with me to ensure my success; special thanks to Dr. Melissa Southwell and Dr. Jessica Veenstra, who introduced me to the wonderful world of pedology through field work and encouraged me to pursue graduate research.
- My advisor, Dr. Judy Turk, for her unwavering support through all the adversities we encountered on this journey and for her understanding that being in good health – mental, emotional, and physical – is paramount for success.
- Wayne Woldt, for helping me get drone imagery needed for my research.
- Les Howard, for helping me create the maps needed for this paper.
- Everyone at UNL's St. Thomas Aquinas Newman Center for giving me a physical space to work and a spiritual space to pray, and Temple Sinai in Atlanta for giving me a spiritual home during the pandemic and for celebrating the little victories with me.

Table of Contents

CHAPTER 1. INTRODUCTION

Hydrologically isolated wetlands, which form at the lowest point in an internally drained basins, contribute many vital ecosystem services such as water filtration and storage, carbon sequestration, and wildlife habitat (Vaughan, DeMoss, Cullum-Muyres, & Diaz, 2020). Several types of hydrologically isolated wetlands are found on the Great Plains and Central Lowlands, including playas (small, ephemeral wetlands of arid and semi-arid environments), salinas (large ephemeral saline lakes), and prairie potholes (depressional wetlands formed in kettles and other glacial settings) (Bowen & Johnson, 2012; Hirmas & Mandel, 2017). The Todd Valley is located at the boundary of the Great Plains and Central Lowlands (USDA-NRCS, 2006). It is an extinct valley of the Platte River in eastern Nebraska and has an incomplete drainage system with numerous small wetlands. These wetlands are often referred to as playas (LaGrange, Stutheit, Gilbert, Shurtliff, and Whited, 2011), though in many ways they are a poor fit with the typical definition of playa wetlands. They occur in a sub-humid climate, are smaller than most playas (<1 to 7 ha, instead of 20 to 50 ha), and are located further east then most playas, which are most abundant in the High Plains region of the Great Plains (Bowen & Johnson, 2015; Tiner, 2003).

Typical playas are closed, shallow basin wetlands (Bowen & Johnson, 2015; Tiner, 2003). They are an important feature of the Great Plains landscape because of the ecosystem services that they provide and their ubiquity. The formation of playas on the High Plains is attributed to either dissolution of underlying carbonates (shallow petrocalcic horizons) or evaporite beds in deeper geologic strata and/or deflation (Bowen & Johnson, 2012). Fluvial, eolian, and pedogenic processes are thought to play a role in evolution of the basins, including dissolution, deflation, and increased ponding of water and episaturation of the soil due to pedogenic accumulation of illuvial clay. Playas also serve as sinks for sediments (Kolodynska-Gawrysiak & Poesen, 2017).

During the late Quaternary period, several environmental changes took place that altered the landscape of the Great Plains and Central Lowlands. Widespread loess deposition occurred during the Middle and Late Pleistocene and Holocene (Mason, 2001; Miao, Mason, Johnson, & Wang, 2007). Loess deposition across pre-existing upland depressions led to smoothing of the terrain (Kuzila & Lewis, 1993). Of the loess units on the Great Plains, late Quaternary Peoria Loess is the thickest and most extensive (Bettis, Muhs, Roberts, & Wintle, 2003).

Soils in deflation basin wetlands in Nebraska are vertic subgroups of Argiaquolls and Argialbolls, including the Lodgepole, Filmore, Scott, and Massie series (Hirmas & Mandel, 2017). The Scott and Fillmore series are both mapped in the Todd Valley (Elder et al., 1965). These soils contain 0.5 to 2% organic carbon and redoximorphic features in the A horizon. The amount of carbon stored in soils is dependent on the relative rates of carbon inputs and outputs of the soil system. Addition of carbon to the soil occurs primarily through the deposition of plant matter. The loss of carbon occurs primarily through respiration by microorganisms that breakdown organic matter in the soil. High net primary productivity and slow decomposition processes under anaerobic conditions in waterlogged soils favor the net accumulation of soil carbon in wetlands (Mitsch et al., 2013). Redoximorphic features are formed by reductive dissolution and subsequent oxidation of iron and manganese compounds (Vepraskas & Vaughan, 2016). Saturated conditions prevent atmospheric O_2 from entering soil (Vepraskas, Polizzotto, & Faulkner, 2016), leading to the use iron and manganese as alternate electron acceptors by anaerobic bacteria (Vepraskas & Vaughan, 2016).

In addition to the redoximorphic features, deflation basin wetlands also contain many subsurface diagnostic features that are distinguish them from the soils of the surround uplands. Albic are a common feature of playa wetlands and are mainly associated with the basin margins, where E

horizons are thicker and deeper in the soil compared to the basin floor (Assmus, 1993). The albic horizons of the basin edge have colors that may easily be confused with a gleyed matrix, formed through redoximorphic processes, but are predominantly influenced by intense leaching and eluviation. Slickensides and wedge-shaped soil structure are frequently apparent in playa subsoils (Hirmas & Mandel, 2017), because of shrink-swell and the high coefficient of liner extensibility inherent in smectitic soil materials (Kuzila & Lewis, 1993; Hartley, Presley, Ransom, Hettiarachchi, & West, 2014). Argillic horizons are typically better expressed in playas than in soils of the surrounding uplands (Kuzila & Lewis, 1993). This may be explained by the greater cumulative moisture flux of the playa basins, but may also be associated with lithologic discontinuities that are better preserved in the aggradational setting of the playas (Kuzila & Lewis, 1993; Mason & Nater, 1994).

The purpose of this study is to: 1) characterize the soil morphology of deflation basin wetlands of the Todd Valley and 2) evaluate carbon and nitrogen storage in the basins. Increased understanding of deflation basin soils will help with efforts to restore and protect critical wetland resources of the Great Plains and Central Lowlands.

CHAPTER 2. MORPHOLOGY AND PARTICLE SIZE DISTRIBUTION OF DEFLATION BASIN SOILS IN EASTERN NEBRASKA, USA

Abstract

Depressional wetlands are a common feature of the Great Plains and Central Lowlands of the United States. Management and restoration efforts to protect wetlands require an understanding of their soils. This study was conducted to characterize and interpret the soil morphology of deflation basin wetlands in eastern Nebraska. Three basins were selected for analysis in the Todd Valley, an abandoned valley of the Platte River. In each basin, three soil cores were collected along three transects from the uplands to the basin floor. The soil morphology of the cores was described and samples from each horizon were collected for particle size analysis. Some soils, mostly at the basin edge, had albic horizons, which were relatively deep in the soil (upper boundary at 34 to 62 cm). Soils of the basin had a higher total mass of clay in the soil profile, but the center of mass of clay in the profile was similar between the uplands and playas. Based on the soil morphology, an estimated 20-30 cm of colluvium occurs in soils of the basin edge, which is less eluviated compared to the underlying horizons, resulting in darker soil color and higher clay content. Soils vary in predictable ways across the deflation basins examined in this study, but also vary between the basins in terms of overall degree of soil development.

Introduction

In the Great Plains and Central Lowlands, depressional wetlands provide wildlife habitat, support biodiversity, mitigate against flooding, filter pollutants, and contribute to nutrient cycling (Bowen & Johnson, 2012, 2017). One common type of depressional wetlands in the region are circular to quasicircular, shallow basins with nearly level bottoms (Bowen, Johnson, Egbert, &

Klopfenstein, 2010). Water enters the wetlands via rainfall and runoff (LaGrange, Stutheit, Gilbert, & Shurtliff, 2011; Tiner, 2003), resulting in episaturation which is reinforced by the low hydraulic conductivity of well-developed argillic horizon that form in the basins.

In the Todd Valley in eastern Nebraska, wetlands tend to be relatively small (<2 ha) compared to similar depressions in the region (LaGrange et al., 2011). These wetlands are distinct from the Rainwater Basins, which are found relatively nearby. The Rainwater Basins are closed basins formed by wind action, and are numerous throughout the level to gently undulating loess plains of south central Nebraska (Kuzila and Lewis, 1993; Stutheit, Gilbert, Whited, & Lawrence, 2004; LaGrange et al., 2011). The Todd Valley deflation basins and Rainwater Basins are both closed depressional wetlands with internal drainage and are significant wildlife habitats (Tiner, 2003). However, Rainwater Basins range in size from 0.5 to 400 ha (LaGrange et al., 2011).

Soils associated with both types of depressional wetlands in Nebraska include the Lodgepole, Butler, Fillmore, Scott, and Massie series (Assmus, 1993; Hirmas & Mandel, 2017), which occupy a cumulative area of 290,039 ha in Nebraska (O'Geen, 2017). These soils are Argialbolls and Argiaquolls, with deeper, thicker argillic horizons compared to the surrounding uplands (Kuzila and Lewis, 1993). Eluvial horizons in the upper part of the profile are light in color and low in pH due to stripping of cations from the grain surfaces (Birkeland, 1999; Bockheim & Gennadiyev, 2000; Turk, Chadwick, & Graham, 2011; Schaetzl & Thompson, 2015). The underlying Bt horizon is characterized by illuvial accumulation, resulting in elevated clay contents, clay films, and iron-manganese concretions, which are the result of oxidation of iron and manganese that has been leached into the illuvial horizon during periods of anaerobic conditions in the surface horizons (Birkeland, 1999; Schaetzl & Thompson, 2015; Vepraskas & Vaughan, 2016). The depth and expression of argillic horizons across the deflation basin

landscape is potentially influenced by cumulative moisture flux, lithologic discontinuities in the loess stratigraphy, and infilling of the basins (Kuzila and Lewis, 1993; Mason and Nater, 1994).

The Todd Valley is a 10-13 km wide, 48 km long loess-mantled, abandoned valley of the Platte River that extends diagonally across Saunders County, Nebraska (Elder et al., 1965). The valley is nearly level with slight swells and swales and an incomplete drainage pattern in which water collects in the swales. Swales throughout the valley comprise a system of seasonally, temporarily flooded, freshwater wetlands, sometimes referred to as the Todd Valley Playa wetlands complex (LaGrange et al., 2011). Soils of the Todd Valley are formed in Peoria Loess, which was deposited approximately 12,000—25,000 years ago (Mason et al., 2003). The basins are thought to originate from deflation into the fluvial sediments of the valley, which were subsequently covered with loess, but still retain relief features that formed in the buried landscape (Stutheit et al., 2004). Mean annual temperature at the site is 9.8ºC and mean annual precipitation is 70.9 cm (Mead6S Station, Eggleston, 2013). The three basins analyzed in this study were 0.2, 2, and 7 ha in area (Fig. 1), with 0-1% slope, less than 1m elevation difference between the playa floor and surrounding uplands. The basins sampled in the study were located on land that is used for pasture, though much of the surrounding land is used for row crop agriculture. The objective of this study is to characterize and interpret the morphology of deflation basin wetland soils in the Todd Valley of eastern Nebraska. This knowledge will contribute to wetland restoration efforts and interpretation of hydrology in the basins.

Methods

Field methods

Three transects were established in each basin, with each transect including a sampling point in the upland, basin edge, and basin floor. The basin floor sampling points were within the boundary that was submerged during initial survey of the site in April of 2019. The basin edge was not submerged, but within the boundary found to meet the Redox Dark Surface indicator for hydric soils. To meet this indicator the soil must have a sufficiently dark matrix color with a certain threshold of redoximorphic concentration abundance and distinctness, which varies depending on the exact matrix color (USDA-NRCS, 2018). The upland points were outside of the hydric soil delineations.

Sampling took place June to October 2019. A Giddings probe was used to take 7.6-cm diameter cores to a depth of 2 meters. Alternatively, for sampling locations that were too wet to access with the truck-mounted Giddings probe, a Geoprobe was used for extraction of 4-cm diameter cores. The sites along the basin floor of Basin 1 could not be reached with the Geoprobe and were sampled instead with an AMS gas powered core sampling kit, also using a 4-cm diameter coring tube. Soil horizons in each core were identified and soil morphology was described according to standard methods (Schoeneberger et al., 2012).

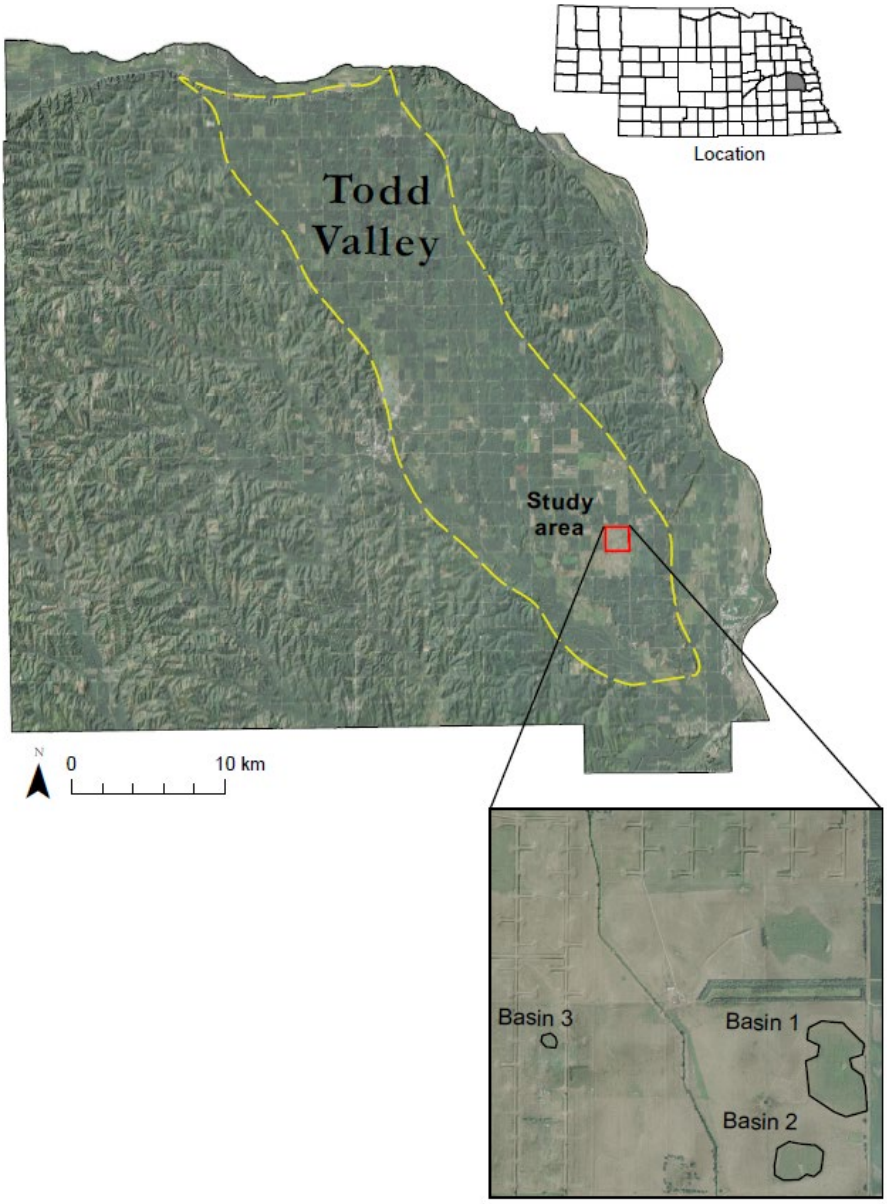

Figure 1: (Top left) Map of the Todd Valley, showing the ENREC boundary and the study area; (inset) the study site with all three basins outlined.

Laboratory methods

Full laboratory analysis was performed on a limited subset of pedons, including all three pedons from the upland and basin edge in basin 1, as well as one pedon from the upland and basin edge in basin 2. Bulk density was determined by the Saran-coated clod method for cores collected using the Giddings probe (Soil Survey Staff, 2014a). This method of sampling produces bulk densities that compare well with clods collected from a soil pit (Airori, Baker, & Turk, In Press). For the cores taken using the Geoprobe and AMS core sampling kit, bulk densities were calculated by weighing 5-cm segments of the cores and calculating volume from the core diameter (Veenstra & Burras, 2015). Particle size distribution was evaluated by the pipette method with standard pre-treatments to remove organic matter and dispersion in sodium hexametaphosphate solution at the Kellogg Soil Survey Lab (KSSL) (Soil Survey Staff, 2014a).

Data analysis

Soil morphology and characterization data were used to classify the soils according to the most recent edition of the Keys to Soil Taxonomy (Soil Survey Staff, 2014b). The amount and distribution of clay in the profiles was summarized by calculating the total mass of clay to 200 cm and center of mass of clay (Presley, Ransom, Kluitenberg, & Finnell, 2004). Total mass to 200 cm (M200) was calculated as

$$M_{200_n} = m_1(z_1) + m_2(z_2 - z_1) + \cdots + m_n(z_n - z_{n-1}) \qquad \text{(eq. 1)}$$

where m_1, m_2, …., m_n are mass per unit volume of clay (calculated by multiply the mass fraction of clay by bulk density) and z_1, z_2,…., z_n represent the thickness of each horizon. The center of mass, d_z (cm), for clay in the profile was calculated as

$$d_z = \frac{1}{2}\left[\frac{m_1(z_1{}^2)+m_2(z_2{}^2-z_1{}^2)+\cdots+m_n(z_n{}^2-z_{n-1}{}^2)}{m_1(z_1)+m_2(z_2-z_1)+\cdots+m_n(z_n-z_{n-1})}\right] \quad \text{(eq. 2)}$$

Particle size distribution data were also analyzed according to the generalized index of soil development, which generates an index based on the relative degree of differentiation between the eluvial and illuvial portions of the profile (Koop, Hirmas, Sullivan, & Mohammed, 2020).

Results

In basin 1, the upland soils had an A horizon that averaged 24 cm thick over several Bt horizons that extended to more than 200 cm (Fig. 2). The upper Bt horizons have mollic colors, which continue to more than 100 cm. Manganese concentrations were observed starting around 80 cm depth and iron concentrations only occurred in the lower Bt horizons (more than 180 cm deep). The maximum clay in the profile was 37.9% and occurred at a depth of 139 to 181cm (Table 1). The basin edge had a thicker A horizon, extending to approximately 47 cm. It could be subdivided into two horizons with subtle differences in color, texture, and root density (Fig. 3), which are labeled in the descriptions as A and Ab (Fig. 2, Table 1). Higher clay was detected in the A (30%) compared to the Ab horizon (17.8%) based on the laboratory analysis (Table 1). Below this is an Eb horizon from 47 to 64 cm, with albic colors. Under that are several Btb horizons from 65 to 160 cm. Mollic colors also occur in the Btb horizons to more than 100 cm depth, though they are not continuous from the surface due to the intervening E horizon. Below the Btb horizons a C horizon with platy structure was observed starting at about 160 cm. Iron and manganese concentration were observed throughout the profile, but were most abundant in the Btb2 and Btb3 horizons. Redox depletions were only observed in the Btb2 and Btb3 horizons. The highest clay in the profile was 43.8% and occurred in the Btb1 horizons (70-120cm) (Table

1). The basin floor soils had a thinner A horizon compared to the basin edge (30 cm on average), with no indication of a buried profile reflected in the morphology. There were E horizons from about 30 to 55 cm. The E horizons were not light enough in color to be albic but did display platy structure. Below this was a Bw horizon (55-73 cm) and Bt horizons (73 to 140 cm). Mollic colors extended from the soil surface to the lower boundary of the Bt horizons in most cases. Below the Bt horizons were a BC and C horizons. Iron concentration and depletions were observed throughout the entire profile in these soils. Clay was estimated to be higher in the Bt horizons of the basin floor compared to the upland and basin edge, but this result was not confirmed by laboratory analysis.

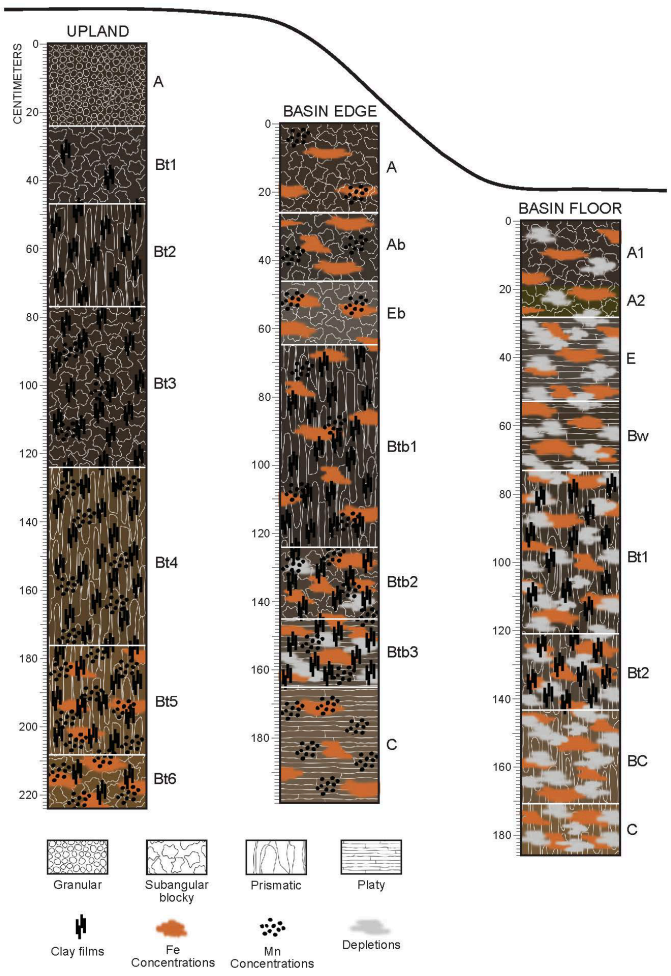

Figure 2: Illustrations of soil profiles in Basin 1. Horizon thicknesses and properties are composites created based on the three transects. Colors used in the background are representations of the Munsell colors recorded in the field.

Table 1. Abbreviated field descriptions and laboratory data for basin 1 transect 1.

Depth	Horizon	Matrix color†	Field texture	Lab texture	Lab sand	Lab clay	Bulk Density‡
cm					----------%----------		g cm^{-3}
			Basin 1 Transect 1 Upland				
0-23	A1	10YR 2/2	sic	sicl	6.5	29.3	1.29
23-45	A2	10YR 2/1	sicl	sicl	4.9	31.3	1.26
45-84	Bt1	10YR 2/2	sic	sicl	4	33.4	1.31
84-106	Bt2	10YR 2/2	sic	sicl	2.8	33.1	1.4
106-139	Bt3	10YR 3/3	sic	sicl	3.1	36.7	1.31
139-181	Bt4	10YR 3.5/3	sic	sicl	4.2	37.9	1.44
181-218	Bt5	10YR 4/3	sic	sicl	5	35.4	1.34
218-230+	BC	10YR 4/4	sic	sicl	4.1	32.5	-
			Basin 1 Transect 1 Basin Edge				
0-38	A	10YR 2/1	sicl	sicl	4	30	1.38
38-52	Ab	10YR 3/1	sicl	sil	4.9	17.8	1.31
52-70	Eb	10YR 4/1	sicl	sil	4.6	15.7	1.49
70-120	Btb1	10YR 2/1	sicl	sic	3.5	43.8	1.4
120-456	Btb2	10YR 3/2	sicl	sic	4.1	43.5	1.46
146-166	Btb3	10YR 4/2	sicl	sic	4.3	42.1	1.44
166-188	C1	10YR 4/2	sicl	sic	4.9	40.5	1.56
188-200+	C2	10YR 4/2	sicl	sicl	4.7	37	-
			Basin 1 Transect 1 Basin Floor				
0-18	Ap	10YR 2/1	sicl	-	-	-	-
18-53	E	10YR 2/1	sil	-	-	-	-
53-73	Bw	10YR 3/1	sicl	-	-	-	-
73-123	Bt1	10YR 2/1	c	-	-	-	-
123-166	Bt2	10YR 2/1	c	-	-	-	-
166-186	BC	10YR 3/2	c	-	-	-	-
186-198+	C	10YR 4/3	sic	-	-	-	-

†The matrix colors given are moist Munsell colors of broken ped faces

‡Clod bulk densities at 33kPa

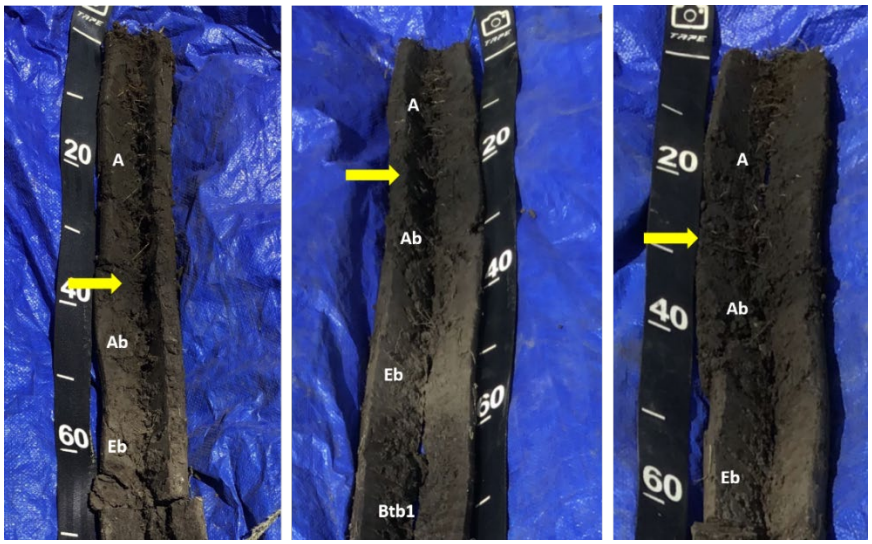

Figure 3:Photos of soil cores from the playa edge of basin 1. Yellow arrows mark the boundary that was interpreted as the original playa surface.

In Basin 2, the upland soils had A horizons that were about 40 cm thick with mollic color (Fig. 4). Below this were Bt horizons from about 40 to 160 cm. Mollic color was observed in the upper Bt horizon to about 65 cm. Manganese concentrations were observed starting at 40 cm, iron concentration starting at 70 cm, and depletions were observed below 100 cm. The maximum clay was 36.4% and occurred at a depth of 139 to 181 cm (Table 2). At the basin edge, the A horizon was about 55 cm thick and had mollic colors. In contrast to basin 1, there were no E horizons observed at the basin edge, though the lower A horizon did have platy structure. Also in contrast to basin 1, the upper A horizon did not have an elevated clay content at the basin edge. Below this A horizon were several Bt horizons from 55 to more than 200 cm depth. The maximum clay was 38.3% and occurred at a depth of 92 to 105 cm. Mollic color continued into the Bt horizons down to about 100 cm. Effervescence with dilute hydrochloric acid was observed in the Bt horizon of one of the cores. Manganese and iron concentrations were observed to the surface and depletions started below 165 cm. The A horizon of the basin floor was about 35 cm

thick and underlain by a thin E horizon (averaging 10 cm) with platy structure, but the color was too dark to be albic. A thin Bw horizon (averaging 10 cm) was observed, and Bt horizons from 65 to 150 cm. Effervescence with dilute hydrochloric acid was observed in the B horizons of one of the cores. Beneath the Bt horizons were BC and C horizons. Mollic colors, iron concentrations, and depletions were observed throughout the entire profile. Comparing the between the three profiles in basin 2, a distinct darkening trend is observed from the upland to the basin floor (Fig. 4).

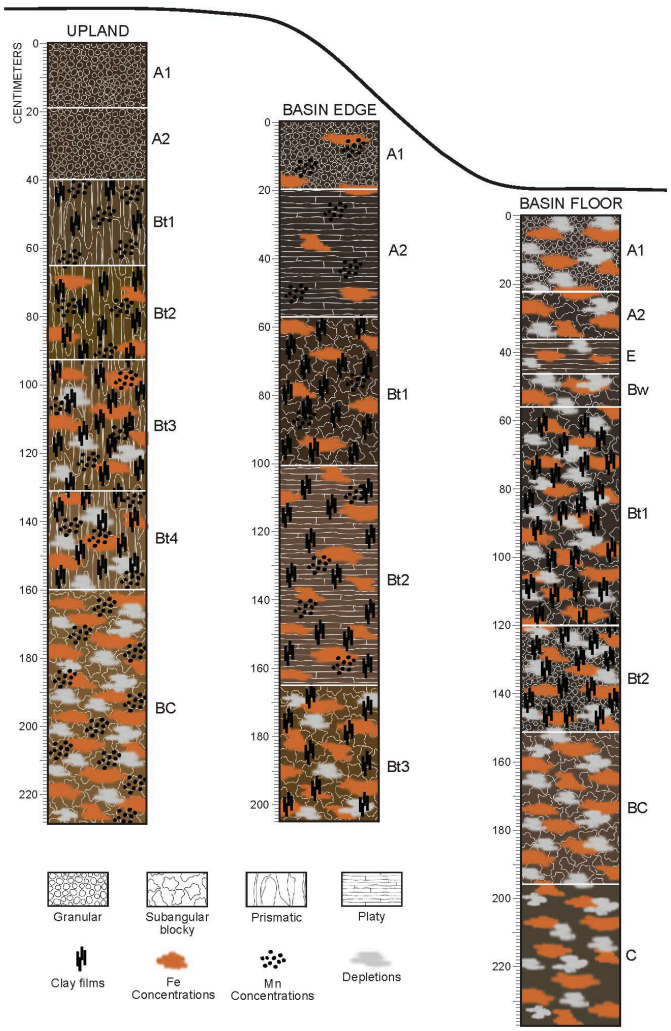

Figure 4: Illustrations of soil profiles in Basin 2. Horizon thicknesses and properties are composites created based on the three transects. Colors used in the background are representations of the Munsell colors recorded in the field.

Table 2. Abbreviated field descriptions and laboratory data for Basin 2 Transects 1/2.

Depth	Horizon	Matrix color†	Field texture	Lab texture	Lab sand	Lab clay	Bulk Density‡
cm					----------%----------		g cm^{-3}
			Basin 2 Transect 1 Upland				
0-19	A1	10YR 2/2	sicl	sicl	6.8	30.3	1.45
19-41	A2	10YR 2/2	sicl	sicl	4.8	34.6	1.31
41-66	Bw	10YR 3/3	sic	sicl	4.3	34.9	1.44
66-92	Bt1	10YR 3/4	sic	sicl	3.4	35.5	1.44
92-135	Bt2	10YR 4/4	sic	sicl	4.9	36.4	1.46
135-166	Bt3	10YR 4/3	sic	sicl	5.6	34.3	1.37
166-195	C1	10YR 4/3	sicl	sicl	4.7	32.4	1.36
195-228+	C2	10YR 4/4	sicl	sicl	5.4	29.9	-
			Basin 2 Transect 2 Basin Edge				
0-22	A1	10YR 2/1	sicl	sicl	4.5	27.8	1.31
22-55	A2	10YR 2/1	sicl	sicl	4.5	32.4	1.24
55-92	Bt	10YR 2/2	sil	sicl	3.7	36.7	1.31
92-105+	Btss	10YR 4/3	sic	sicl	4.2	38.3	1.31
			Basin 2 Transect 1 Basin Floor				
0-17	A1	2.5YR 2.5/1	sil	-	-	-	-
17-31	A2	5YR 2/1	sil	-	-	-	1.43
31-44	E	2.5Y 2.5/1	sil	-	-	-	2.04
44-57	B2	10YR 2/1	sicl	-	-	-	1.55
57-77	Bt1	10YR 2/1	sicl	-	-	-	2.31
77-110	Bt2	10YR 2/2	sicl	-	-	-	2.09
110-119	Bt3	5Y 2.5/1	sicl	-	-	-	2.04
119-136	Bt4	5Y 2.5/1	sicl	-	-	-	2.12
136-183	BC	10YR 3/3	sicl	-	-	-	1.90
183-223+	C	2.5Y 2.5/1	sicl	-	-	-	-

†The matrix colors given are moist Munsell colors of broken ped faces
‡Upland and Basin Edge: Clod bulk densities at 33kPa, Basin Floor: Core segment bulk densities

In Basin 3, the upland soils had an A horizon from 0 to 15 cm and AE horizons with platy structure from 15 to 25 cm (Fig. 5). Below the AE horizon was an Ab horizon with platy structure and 10YR 2/1 colors from 25 to 52 cm, a Bwb horizon from 52 to 77 cm, and several Btb horizons from 77 to more than 200 cm. Mollic color extended into the Btb horizons, down

to about 155 cm. Manganese and iron concentrations, as well as depletions, were observed in horizons below 130 cm. At the basin edge the A horizons were 49 cm thick. These horizons were labeled as A1 and A2 due to limited distinction in color, but could potentially be interpreted as a buried surface beneath younger colluvium (A and Ab). Beneath the A horizons was an E horizon with platy structure and albic color from 49 to 69 cm and several Bt horizons extending to more than 200 cm depth. Mollic colors occurred throughout the profiles except for the E horizons. Iron and manganese concentrations and depletions were observed throughout the profiles. The basin floor had an A horizon that was 34 cm thick and an E horizon from 34 to 48 cm, which had platy structure but color that were too dark to be albic. Several Bt horizons were observed from 48 cm to 158 cm and a C horizon with platy structure was beneath the Bt horizons. Mollic color, iron and manganese concentrations, and depletions were observed throughout the profile.

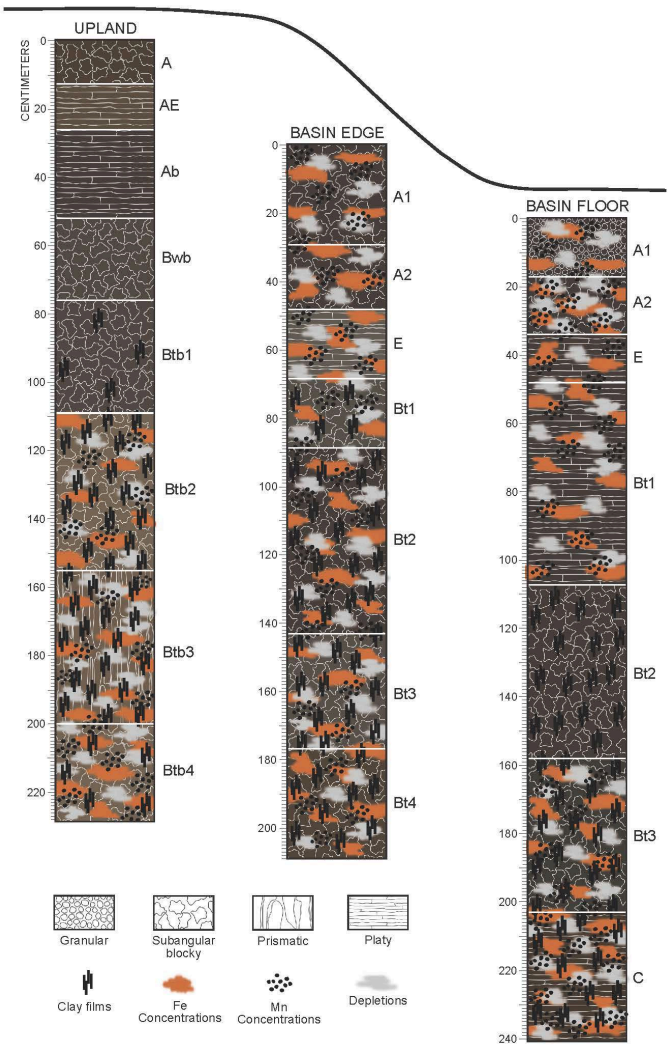

Figure 5: Illustrations of soil profiles in Basin 3. Horizon thicknesses and properties are composites created based on the three transects. Colors used in the background are representations of the Munsell colors recorded in the field.

Table 3. Abbreviated field descriptions and laboratory data for basin 3 transect 1.

Depth	Horizon	Matrix color†	Field texture	Bulk Density‡
cm				g cm^{-3}
		Basin 3 Transect 1 Upland		
0-11	A1	10YR 2/2	sicl	-
11-28	A2	10YR 2/1	sicl	-
28-47	A3	10YR 2/1	sicl	-
47-76	A4	2.5Y 3/1	sicl	-
76-121	Bt1	10YR 3/1	c	-
121-168	Bt2	10YR 3/1	c	-
168-195	Bt3	10YR 3/1	sic	-
195-220+	C	10YR 4/1	sic	-
		Basin 3 Transect 1 Basin Edge		
0-17	A1	10YR 2/1	sicl	-
17-34	A2	10YR 2/1	sil	-
34-63	E	10YR 3.5/1	sil	-
63-90	Bt1	2.5Y 3/1	sic	-
90-151	Bt2	10YR 2/1	c	-
151-186	Bt3	10YR 2/1	sic	-
186-208+	Bt4	10YR 3/1	sic	-
		Basin 3 Transect 1 Basin Floor		
0-11	A1	N 2.5/-	sil	1.27
11-24	A2	N 2.25/-	sil	1.07
24-35	E	2.5Y 2.5/1	sil	1.63
35-98	Bt1	10YR 2/1	sic	1.84
98-142	Bt2	10YR 2/1	sic	2.00
142-216	Bt3	10YR 2/1	sic	1.86
216-248+	BC	10YR 2/2	sicl	

†The matrix colors given are moist Munsell colors of broken ped faces
‡Core segment bulk densities

Overall, morphologic features of soils in the Todd Valley wetlands complex include albic horizons, argillic horizons, redoximorphic features, and effervescence with 1N HCl (Table 1). Albic horizons occurred most frequently at the basin edge, where they occurred in two of the three transects in basins 1 and 3. Some soils on the basin floor had E horizons, but only one of these in soils (in basin 1) met the color requirements for an albic horizon. The association of albic horizons with the perimeter of playa wetlands is consistent with previous studies in the Rainwater Basins (Assmus, 1993). However, the albic horizons observed in the Basins 1 and 3 were deeper and thicker than those typically associated with playa wetlands of the region. The upper boundary of the albic horizon occurred at 42-52 cm in Basin 1 and 34-64 cm in Basin 3, which are both considerably greater than depth of the albic horizons described at Massie lagoon in the Rainwater Basins (15-30cm) and the upper boundaries of albic horizons in the official series descriptions of the Fillmore, Scott, and Massie series (13-23cm) (Assmus, 1993; Soil Survey Staff, 2019). The thickness of the albic horizon was 16-18cm in basin 1 and 12-29 cm in basin 3, also greatly exceeding the 5-10cm albic horizons observed in the rainwater basins and reflected in the official series descriptions of the Argialbolls associated with playa wetlands of the regions. Basin 2 had no soils with albic horizons and was the only basin which had horizons showing effervescence in response to 1N HCl, indicating the presence of calcium carbonate. This may be due to the flocculating effect of calcium ions in the soil, preventing the dispersion of clay particles required for formation of the albic horizons. Alternatively, the presence of carbonates and the absence of albic horizons may both be explained by less leaching in this basin. Argillic horizons were present in all profiles described at the basin edge and basin floor, and most soils of the uplands (Table 1).

Redoximorphic features were observed closer to the surface in the basins relative to the uplands, as expected (Vepraskas & Vaughan, 2016). The shallowest redoximorphic features were observed at 38 to 181cm in the uplands and 0 to 92 cm in the basins (Table 1). Redoximorphic features were observed at the surface in all basin floor profiles, but the depth to such features at basin edges varied considerably from site to site.

Table 4. Summary of profile characteristics observed along transects in the three basins.

	Basin 1			Basin 2			Basin 3		
	Upland	Basin edge	Basin floor	Upland	Basin edge	Basin floor	Upland	Basin edge	Basin floor
Albic horizon									
Presence	0/3	2/3	1/3	0/3	0/3	0/3	0/3	2/3	0/3
Upper boundary (cm)		48-52	37					34-62	
Thickness (cm)		16-18	24					12-29	
Argillic horizon									
Presence	1/3	3/3	3/3	2/3	3/3	3/3	3/3	3/3	3/3
Upper boundary (cm)	106	60-70	73-136	38-92	49-59	48-61	76-105	63-86	35-60
Thickness (cm)	112	94-111	11-93	43-115	41-100	78-112	106-119	80-145	120-180
Redoximorphic features									
Upper boundary (cm)	87-181	0-92	0	38-166	0-55	0	90-121	0	0
Effervescence									
Presence in profile	0/3	0/3	0/3	0/3	1/3	1/3	0/3	0/3	0/3

Using data from laboratory particle size analysis, the increased development of argillic horizons in the basins compared to the surround uplands becomes apparent. The total mass of clay in the upper 2m of soil was found to be higher in the basin compared to the upland, indicating greater production of clays in the basin (Table 5). However, the extent of clay translocation, as reflected in the depth of the center of mass for clay was only slightly higher in the basin (mean = 111cm) compared to the surrounding uplands (mean = 105 cm).

Table 5. Average and standard error total clay and center of mass for clay in the upper 200 cm of soil in Basin 1.

	Upland	Basin Edge
Total clay $M_{200,}$ kg m^{-2}	880 (38)	1065 (24)
Total clay d_{200}, cm	105 (1)	111 (3)

The particle size distribution data can also be used to interpret patterns of soil development in the basin through use of the generalized index of soil development, which rates overall soil development based on the relative differences detected between the eluvial (A and E) and illuvial (B) horizons (Koop et al., 2020). The first step in evaluation of the generalized index of soil development for particle size distribution is calculating the geometric mean particle size diameter for each horizons (Figs. 6A, 7A). In a well-developed soil profile, this value should be higher, indicating coarser textures, in the eluvial horizons and lower, indicating finer textures, in the illuvial horizons (Koop et al., 2020). This pattern is well illustrated in the upland of basin 1 (Fig. 6A) and the edge of basin 2 (Fig. 7A). There is a more complex pattern at the edge of basin 1 (Fig. 6A), where fine textures were observed in the upper two A horizons. In the upland soils of basin 2 (Fig. 6A), coarser textures are encountered in the C horizon, supporting the characterization of this horizon as being beyond the depth of significant illuvial accumulation.

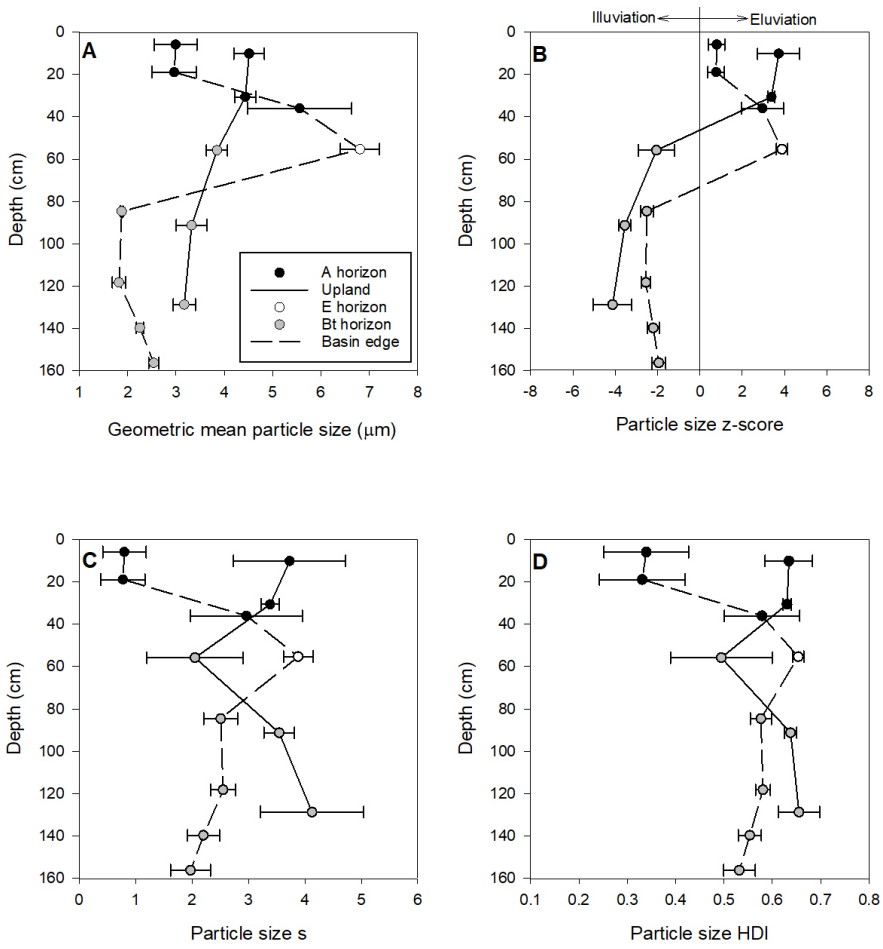

Figure 6: Components of the generalized index of soil development for particle size calculated in basin 1: A) geometric mean particle size diameter, B) particle size $\tilde{z}$-score, C) particle size score (S), and D) particle size horizon development index (HDI). Error bars indicate standard error of the mean for the three transects. Position of the points on the y access represents the mid-point of each horizon, averaged between the three transects in the basin.

The particle size $\tilde{z}$-score reflects the relative difference between the particle size of the eluvial and illuvial horizons, with more positive values corresponding to greater eluviation and more negative value corresponding to greater illuviation. This pattern can bet seen by comparing and A and E horizons (positive values) with the B horizons (negative values), while C horizons (observed in basin 2) fall close to 0 (Figs. 6B and 7B). The final steps in finding the generalized index and calculating the score (S), which rates development in relation to the dominate process (eluviation or illuviation) thereby eliminating negative values, and horizon development index

(HDI), which scales the values from 0-1 using an estimate of the total range of values obtained through analysis of many pedons form the National Soil Information System database (Koop et al., 2020). In basin 1, the HDI is lower at the basin edge compared to the uplands for most horizons, especially in the upper two A horizons (Fig. 6D). In contrast, basin 2 displays a slightly higher HDI throughout the profile at the basin edge compared to the upland (Fig. 7D).

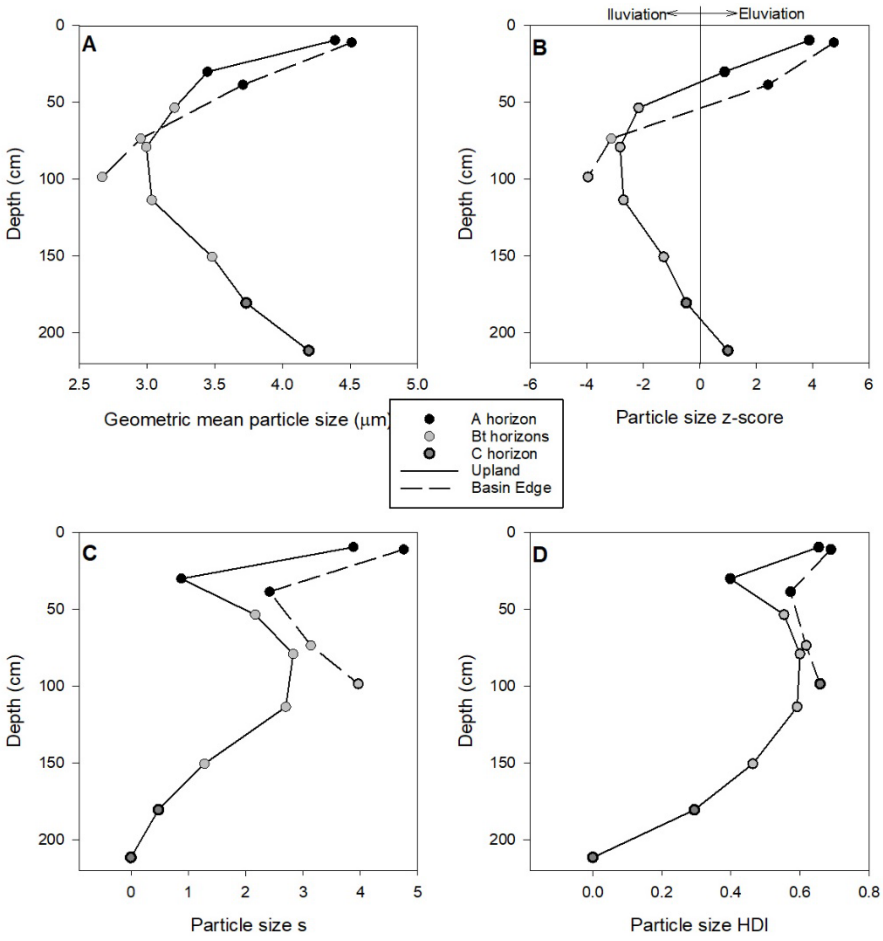

Figure 7: Components of the generalized index of soil development for particle size calculated in basin 2: A) geometric mean particle size diameter, B) particle size z̃-score, C) particle size S, and D) particle size horizon development index (HDI).

Discussion

Results of the HDI calculation in Basin 1 suggest that the upper two horizons of the basin edge profile are formed in younger sediment, possibly derived from erosion of the surrounding

uplands. This layer of younger sediment is approximately 26 cm thick, based on the HDI profile (Fig. 3D). Assuming that the E horizon was developed before this sediment accumulated in the basin, its original upper boundary should be located at 22 to 24 cm, which is within the range of E horizon depths observed in Massie Lagoon (Assmus, 1993), and similar to the reported depths of albic horizons in Fillmore soils. This process also warrants consideration in interpreting data on clay accumulation and transport in the basin (Table 6). A portion of the accumulated clay is possibly derived from transport of fine-texture sediments into the basin through erosional processes (Bowen and Johnson, 2017), accentuating the contrast in M_{200} between the upland and the basin edge. This process would also shift the center of mass for clays upward in the profile (leading to a higher d_{200}), consequently masking degree of illuvial transport of clays in basin edge soils.

The significance of erosion and deposition processes in the basins raises questions regarding the best horizon nomenclature for describing such profiles. A conventional description of this profile might be A1/A2/A3/E/Bt1/Bt2/Bt3/Bt4 (*e.g.*, Fig. 2, basin floor profile), alternatively A1/A2/Ab/Eb/Btb1/Btb2/Btb3/Btb4 might be better for communicating the depositional processes in the basin (*e.g.*, Fig. 2, basin edge profile), especially the formation of the buried horizon prior to accumulation of sediments that form the upper part of the A horizon. It might also be appropriate to include a prefix numbering in the profile (A1/A2/2Ab/2Eb/2Btb1/2Btb2/ 2Btb3/2Btb3), indicating the difference in transport processes from which the parent material is derived (i.e., colluvium over loess).

Current conventions for describing soil profiles make it difficult to discern the soil scientist's interpretation of process and potential loss of playa storage volume, which is critical to guide restoration efforts (Bowen and Johnson, 2017). However, discerning the original surface presents

a challenge. Observations presented in this study suggest that there is only a subtle color difference. The original playa surface may be slightly lighter (one unit higher in value) in color compared to the overlying A horizons presumed to be formed in colluvial sediments (Figs. 2, 3, 5). Texture is the most important distinction between these layers. Upper A horizons (presumed colluvium) have silty clay loam textures (30-35% clay), while silt loam textures (18-21% clay) characterized the lower part of the A horizon (presumed loess) (Tables 1, 3). Lastly, though we did not quantify the difference, there is a noticeable decrease in root density visible in our field photographs, which also serves as a marker of what we interpret as the original playa surface (Fig. 3). Root density is indicative of differences between horizons that impact conditions for plant growth, such as a physical restrictive layer (Drohan, Thompson, Lindbo, Beaudette, & Dadio). In the case of the soils examined in the study, the upper A horizon may support more roots because it is less leached and there for retains more plant essential elements. These morphologic indicators of the original surface are considerably different from those used in studies of playas in Kansas (Bowen and Johnson, 2017). In the Kansas playas, a much stronger contrast and inverse pattern in colors was observed, with the playa surface was found to be of lower value and chroma (10YR 3/1) compared to the overlying sediments (10YR 4/3). The pattern in texture was also noted to be the inverse of what we observed, with the playa surface being distinguished by an increase in clay. Several factors may account for the differences, including the nature of upland soils from which colluvial sediments in the basins are derived, the size of the basins, and the current land use.

Conclusions

Our research shows some similarities with studies of deflation basin soils. Albic horizons were not observed in the upland and were most prevalent at the basin edge. Most E horizons on the basin floor did not meet the color requirement to be albic horizons. Argillic horizons also generally showed stronger expression within the basins. One of the playas (basin 2), had no albic horizons in any part of the basin. This may be related to the presence of $CaCO_3$ in basin 2, either because there is greater flocculation and therefore less transport of clays, or lower cumulative moisture flux resulting in reduced transport of both clays and carbonates. In two of the basins (Basins 1 and 3), our interpretation of the morphology suggests 20-30 cm of colluvial sediment accumulation at the basin edge, leading to excessively deep albic horizons (34-62 cm) and a layer of sediments that are slightly darker in color, higher in clay, and supports more roots compared to the horizon that we interpret as the buried surface.

CHAPTER 3. CARBON AND NITROGEN STOCKS OF DEFLATION BASIN WETLANDS IN EASTERN NEBRASKA, USA

Abstract

Wetland soils are important sinks for atmospheric carbon, but this important pool is insufficiently quantified. This study was conducted to compare carbon and nitrogen stocks between the upland, basin edge, and basin floor of wetlands in eastern Nebraska. This work was conducted in two deflation basin wetlands in Nebraska's Todd Valley. Carbon and nitrogen stocks were evaluated to two meters depth using cores collected along three transects from the upland to the basin floor in each wetland. Each basin examined showed a different trend with respect to carbon and nitrogen stocks, one basin had the highest carbon in nitrogen stocks in the upland soils, one basin revealed the highest carbon and nitrogen stocks in the basin floor soils, and another showed not significant difference in carbon and nitrogen stocks along the transects. Morphology of the soils and profile distributions of carbon suggest that the limited carbon storage in these playa wetlands, at least in part, are due to leaching loses of dissolved organic carbon. Compared to other depressional wetlands in the region, the deflation basins of eastern Nebraska show a limited capacity to accumulate organic matter and store carbon.

Introduction

Human impacts on the soil carbon cycle are in many ways intertwined with increasing greenhouse gas concentration and resultant climate change (Amundson et al., 2015). Soils represent the largest terrestrial reservoir of organic carbon, with an estimated 2300 Gt in the upper 3 m of earth's soils (Jobbagy & Jackson, 2000). This amount is more than twice that of the carbon stored in vegetation or the atmosphere (Bellamy, Loveland, Bradley, Lark, & Kirk,

2005). Due to the large size of the soil carbon pool, the balance between the formation and loss of soil organic carbon (SOC) is a major driver of carbon-climate feedbacks (Bellamy et al., 2005; Waring et al., 2020). The balance between inputs of carbon from plants and release of CO_2 by soil respiration as plant matter decomposes ultimately determines the amount of SOC stored in soils (Amundson et al., 2015). Erosion and tillage are major contributors to the redistribution of SOC across landscapes (Ritchie et al., 2006). Tillage accelerates the breakdown of labile carbon, resulting in a lower level of SOC that reaches an approximate steady state after several decades of cultivation (Guo & Gifford, 2002; Stockmann et al., 2013). Erosion has been demonstrated in some settings to increase carbon storage at the landscape scale, by moving SOC from the uplands to wetter lowland settings, where it breaks down slower (Berhe Harte, Harden, & Torn, 2007), though land degradation costs resulting from erosion far outweighs the climate benefits of increased carbon storage (Amundson et al., 2015). Some studies have linked climatic warming to increased soil respiration and widespread loss of carbon from soils (Bellamy et al., 2005).

Wetlands are critical sinks for soil carbon, covering only 5 to 8% of earth's land area, but storing an estimated 20-30% of the global soil organic carbon pool (Lal, 2008; Mitsch & Gosselink, 2007). Considering the wide variety of wetland types, which can vary tremendously in their ability to sequester carbon (Mitsch et al., 2013), more data is needed on carbon storage in regionally important wetland types. Playas and deflation basins are a type or prairie wetland that are widely disturbed throughout the Great Plains and Central Lowlands (Hirmas and Mandel, 2017). However, even extensive compilations of data carbon sequestration in wetlands sometimes fail to consider this type of wetland (Mitsch et al., 2013).

Deflation basins are common throughout in the Todd Valley, which runs diagonally across Saunders County in eastern Nebraska. The Todd Valley is an abandoned valley of the Platte

River, which is 10-13 km wide and 48 km long (Elder, Beesley, & McKinzie, 1965). Soils of the Todd Valley are formed in Peoria loess, which mantles the underlying alluvium. An incomplete drainage pattern characterizes the valley, with numerous swales that collect water. These swales make up the Todd Valley Playa wetland complex, a system of seasonally, temporarily flooded, freshwater wetlands (LaGrange et al., 2011). The formation of the basins is attributed to deflation (Stutheit et al., 2004). However, deflation is thought to have occurred in the alluvial sediments of the Todd Valley, prior to Peoria Loess deposition. Thus, the relief of the basins affects the soils formed in the loess, but the loess itself did not experience deflation.

Aside from slight swells and swales, the relief is nearly level. The three deflation basins considered in this study have less than 1m elevation difference between the basin floor and surrounding uplands, 0-1% slope, and are located on land used for pasture (Fig. 1). Morphologic features of the soils include albic horizons (observed at the edge of basins 1 and 3), argillic horizons which were best expressed in the basins relative to the uplands, diffuse carbonates (only detected in basin 2), redoximorphic features which were closer to the surface in the basins compared to the uplands, and dark, mollic colors that sometimes extended to more than 2 m depth in the basins (see chapter 2). Basins 1 and 3 also show evidence 20 to 30 cm of colluvial infilling along the basin edge.

In depressional wetlands formed in kettle holes, average SOC stock increase from the upland to the center of the wetland (Nitzsche et al., 2017). It can be reasonably hypothesized that a similar pattern will be observed in the deflation basin wetlands of the Todd Valley. The objective is this study is to compare the carbon and nitrogen stocks of the upland, edge, and basin floor components of deflation basin wetlands in eastern Nebraska.

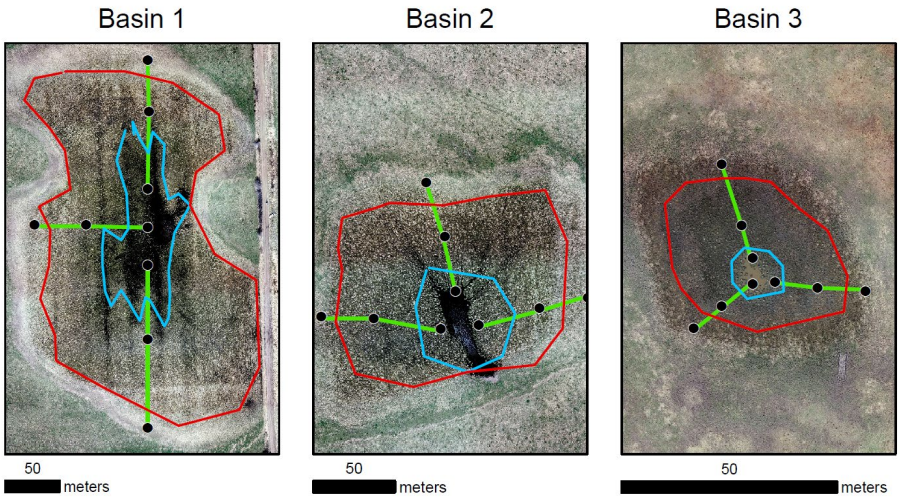

Figure 1: Aerial images of the three basins, delineations of the basin floor and basin edge, and the sampling transects.

Methods

Field methods

The upland, basin edge, and basin floor were sampled along three transects in each basin (Fig. 1). Initial survey of the site in spring of 2019 established the boundary of the submerged portion of the basins. All basin floor sampling locations were within this boundary. The basin edge was considered as the portion of the basin that met the Redox Dark Surface indicator for hydric soils (USDA-NRCS, 2018), but was not submerged at the time of initial survey of the site. Areas outside of the hydric soil delineations were considered as uplands. Cores were collected to 1 to 2.5 m depth at each transect point using a truck-mounted Giddings probe with a 7.6-cm soil tube, a Geoprobe with a 4-cm soil tube, or an AMS gas powered core sampling kit with a 4-cm soil tube. The Geoprobe and AMS core sampling kit were used only in locations that were too wet to access with the truck. Bulk samples were collected by morphologic horizons for carbon and

nitrogen analysis. Intact samples were also collected from each horizon for bulk density analysis in the form of clods (from the 7.6-cm cores) and 5-cm section (from the 4-cm cores). Clods were Saran-coated in the field for transport to the laboratory.

Laboratory methods

Where intact clods could be collected, the clod method was used for bulk density analysis (Soil Survey Staff, 2014a). Clod volumes were measured at both -33kPa and in the oven dry state (dried at 105ºC). Clod bulk densities have been demonstrated to produce more accurate carbon stocks relative to bulk densities calculated from core volume (Gross & Harrison, 2018). Though clods are conventionally collected when sampling a soil pit, the method of collecting clods from a soil core has been shown to result in only minor variations in bulk density results compared to clods collected from a soil pit (Airori, Baker, & Turk, In Press). Furthermore, the differences in bulk density between the core- and pit-derived clods has no significant impact on resultant carbon stock calculations. In locations where only narrower cores could be extracted, the core volume was used for the bulk density calculations, according to the dry mass of the 5-cm sections collected from each horizon, a method which has been used in other studies (Veenstra & Burras, 2015).

Carbon and nitrogen concentrations were measured by dry combustion. Bulk samples were crushed using a soil grinder, then sub-samples were ground to a fine power in a soil mill. A microbalance was used to weigh out 30 to 40 mg samples of the powdered soil, which were wrapped into tin capsules and analyzed by dry combustion on a C/N analyzer (Thermo Flash

2000). Dry combustion was performed in triplicate for quality assurance purposes (Streeter & Schilling, 2015).

Data Analysis

Carbon and nitrogen stocks were calculated to a depth of 2 m for each of the soils sampled. The elemental stock is the mass per area expression of an element within the soil and is the preferred expression for cross-site comparisons (Boone, Grigal, Sollins, Ahrens, & Armstrong, 1999). Carbon and nitrogen stocks were calculated according to the formula:

$$\frac{M}{A} = \sum_{i=1}^{n}(T_i \times \rho_{bi} \times f_i) \qquad \text{(eq. 1)}$$

where M = mass in kg, A = area in m^2, n = number of horizons in the soil, T_i = thickness of horizon i (in m), ρb_i = bulk density of horizon i (in kg m^{-3}), and f_i = fraction of sample mass composed of carbon or nitrogen (Turk & Graham, 2009).

Five of the 18 cores collected from the two basins were less than 2 m deep, so the calculation could not be carried out to 2 m with the data available. For these, the average data from the other two transect points in the same landscape position of the same basin were used to estimate the lower part of the profile that was missing. In some cases, bulk densities were not available at the time of this report. For those horizons, including most of Basins 2 and 3, bulk density was estimated as the average all analyzed samples sharing the same horizon designation at the site (A = 1270 kg m^{-3}, E = 1460 kg m^{-3}, Bt = 1400 kg m^{-3}, C = 1460 kg m^{-3}). One-way ANOVA was performed to compare the carbon and nitrogen stocks of the upland, basin edge, and basin floor within each of the basins using Minitab 18.

Results

At the surface of basin 1, the highest carbon and nitrogen concentrations occur in the soils of the basin floor (Fig. 2). However, this pattern changes with depth. In the lower A, E, and Bt horizons, the soils of both the basin edge and basin floor have lower carbon and nitrogen concentrations compared to the upland. As a result of this difference in the subsoils, the carbon and nitrogen stocks of this basin are highest in the uplands and lower in the soils of the basin (Tables 1, 2). The difference between the soils of the upland, basin edge, and basin floor is nearly significant for the carbon stocks ($p = 0.061$) (Table 1) and significant for the nitrogen stocks ($p = 0.003$).

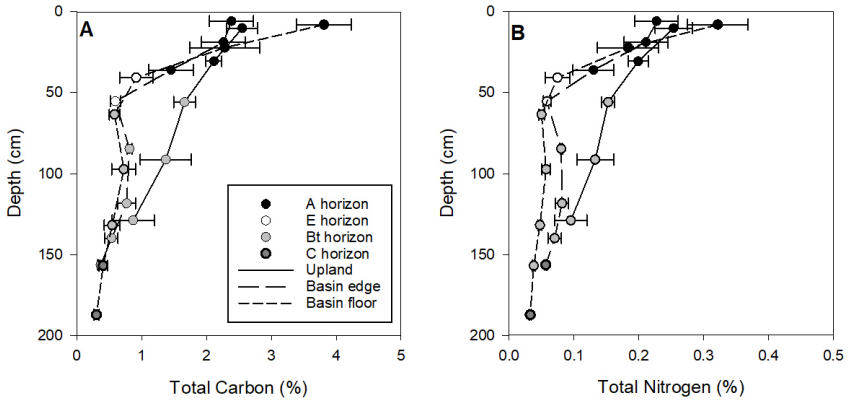

Figure 2: Concentrations of A) total carbon and B) total nitrogen with depth in Basin 1. Error bars indicate standard error of the mean for the three transects. Position of the points on the depth access represents the mid-point of each horizon, averaged between the three transects in the basin.

Table 1. Average and standard deviation of carbon stocks (kg m^{-2}) in the upper 200 cm of soil. P-Values are results of ANOVA comparisons between the upland, basin edge, and basin floor. Values in parentheses are one standard deviation of the mean.

	Upland	Basin Edge	Basin Floor	P-Value
Basin 1	32.4 (2.7)	24.2 (3.3)	25.8 (4.3)	0.061
Basin 2	20.2 (2.0)	29.16 (9.0)	28.4 (3.9)	0.190
Basin 3	28.2 (3.9)	27.5 (2.5)	40.8 (7.7)	0.033

Table 2. Average and standard deviation of nitrogen stocks (kg m^{-2}) in the upper 200 cm of soil. P-Values are results of ANOVA comparisons between the upland, basin edge, and basin floor. Values in parentheses are one standard deviation of the mean.

	Upland	Basin Edge	Basin Floor	P-Value
Basin 1	3.2 (0.2)	2.5 (0.3)	2.2 (0.2)	0.003
Basin 2	2.1 (0.1)	2.6 (0.8)	2.4 (0.2)	0.493
Basin 3	2.2 (0.4)	2.1 (0.2)	3.1 (0.8)	0.078

In basin 2, the highest carbon and nitrogen concentrations were observed at the basin edge (Fig. 3). The basin edge soils show higher carbon and nitrogen concentrations compared to the upland and the basin floor throughout the A horizons, which is more than 50 cm thick. Comparing between the basin floor and the upland, the pattern shows some similarity to those observed in basin 1, with a much steeper drop off in carbon and nitrogen in the lower A and upper Bt horizons on the basin floor, while the upland profile displays a more gradual decrease in carbon and nitrogen with depth. However, the contrast between the upland and the basin floor is much less than seen in basin 1. Results of the ANOVA comparison show insignificant differences for both carbon ($p = 0.190$) and nitrogen ($p = 0.493$) stocks between the upland, basin edge, and basin floor of basin 2 (Tables 1, 2).

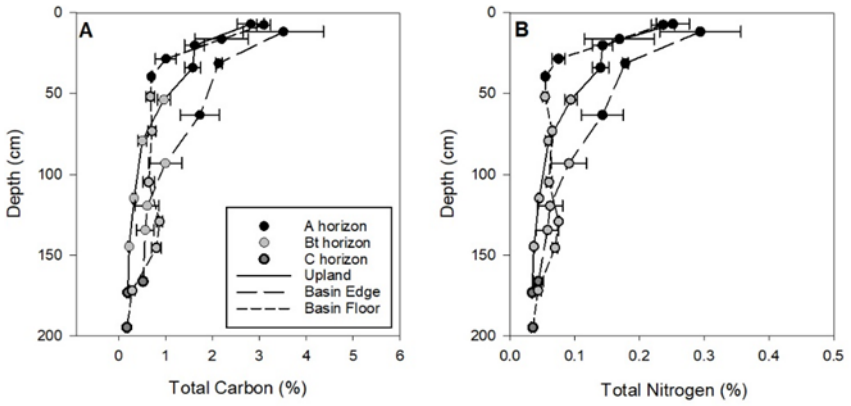

Figure 3: Concentrations of A) total carbon and B) total nitrogen with depth in Basin 2. Error bars indicate standard error of the mean for the three transects. Position of the points on the depth access represents the mid-point of each horizon, averaged between the three transects in the basin.

In basin 3, the E horizons of the basin edge and basin floor had lower carbon and nitrogen concentrations compared to the lower part of the A horizon in the upland (Fig. 4). This echoes the same pattern of carbon and nitrogen being lowered in the E (or lower A) of the basin soils compared to the upland, as seen in the other basins (except for the basin edge soil in basin 2). However, there is one big difference in basin 3, which is the peak in carbon and nitrogen concentrations seen at 120 cm in the basin floor soils. This reflects a high concentration of carbon and nitrogen seen in just one of the basin floor soils at this depth, which is most likely evidence of a well-developed buried soil. The 120 cm peak in carbon and nitrogen was large enough to result in a significantly higher carbon stock ($p=0.033$) and nearly significantly higher nitrogen stock ($p=0.078$) for the basin floor soils of basin 3 (Tables 1, 2).

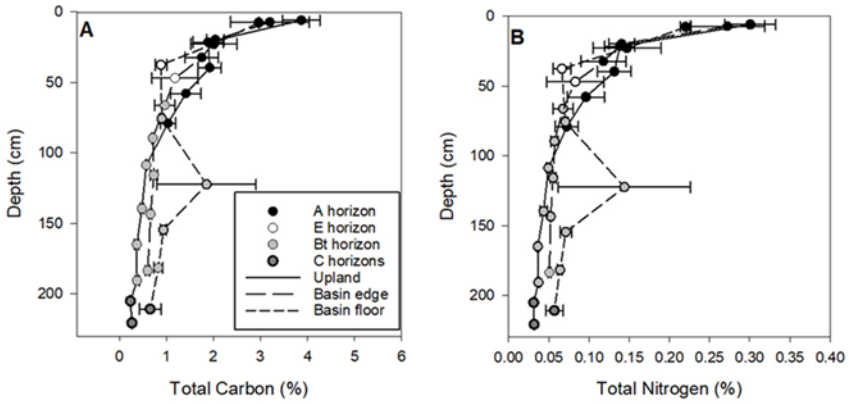

Figure 4: Concentrations of A) total carbon and B) total nitrogen with depth in Basin 3. Error bars indicate standard error of the mean for the three transects. Position of the points on the depth access represents the mid-point of each horizon, averaged between the three transects in the basin.

Discussion

Carbon stocks observed in this study suggest relatively little accumulation of SOC in deflation basins of the Todd Valley. Carbon and nitrogen stocks were found to be higher in the upland compared to the basin (basin 1) or have no significant difference between the upland and basin soils (basin 2) (Table 1, 2). Basin 3 did have significantly higher carbon stocks in the basin floor, but this was attributable to the presence of a buried soil, rather than pedologic processes occurring at the surface of the wetland (Fig. 4, Table 1). This stands in contrast to other depressional wetlands, such as prairie potholes, where carbon increases from the upland to the center of the basin (Nitzsche et al., 2017).

The range of carbon in the upland soils (20.2-32.4 kg C m^{-2}) (Table 1), is slightly high for grassland soils, which average 13.3 kg C m^2 (Post, Emanuel, Zinke, & Stangenberger, 1982). This is as expected, given the relatively high rainfall of the region, which is 710 mm (Eggleston, 2013), compared to 250 to 500 mm range associated with grasslands in the global model of carbon by life zone (Post et al., 1982). However, the wetland soils of the basin have carbon

stocks that are low (24.2-40.8 kg C m^2) (Table 1) compared to other wetland soils, which average 72.3 kg C m^2 (Post et al., 1982). However, the carbon stocks measured in this study are similar to those of the Rainwater Basins in south central Nebraska, which have been calculated as 21.2 to 24.4 kg C m^2 in basin edge positions (Airori et al., In Press). In contrast, prairie potholes, another distinct wetland type of the Great Plains and Central Lowlands (Hirmas & Mandel, 2017), can store as much as 111 to 161 kg C m^2 (Streeter & Schilling, 2015).

The profile distributions of carbon and nitrogen suggests an explanation of low carbon and nitrogen stocks at the basin edge (Fig. 2-4). Generally, the biggest differences between the upland and basin edge soils, in both carbon and nitrogen concentrations, occurs in the E horizons. This suggests that leaching of dissolved organic matter is causing organic matter loss from the basin. In basin soils that lack E horizons (i.e., basin edge of basin 2), carbon and nitrogen concentration are not lowered in the subsoil as they are in the other basin soil profiles (Fig. 3). Intense leaching losses of organic matter from the basin soils may explain why they store relatively little carbon and nitrogen, despite evidence of saturation and anaerobic conditions that would otherwise be expected to lead to high carbon and nitrogen stocks. This process may not be unique to the Todd Valley deflation basins, as data from the Rainwater Basins also offers example of soils with higher organic carbon concentrations in the uplands compared to the basins (Kuzila and Lewis, 1993).

The buried soil encountered in Basin 3 on carbon storage, though only observed in a single core from the basin, is also a notable feature. It suggests some potential for carbon storage in the deflation basin wetlands when we consider the combination of geomorphic processes (loess deposition) and pedologic processes (carbon accumulation). It is often reported that while color and other evidence of buried A horizons may persist in loess, the organic matter is rapidly

oxidized and lost following burial (Busacca, 1989; Hallberg, Wollenhaupt, & Miller, 1978; Khormali & Kehl, 2011). However, the presumed buried soil encountered in Basin 3 contains more than 3% organic carbon. The persistence of organic matter in this buried soil is likely attributable to the anaerobic conditions and resultant slow decomposition of organic matter in the basin. However, this buried A horizon was difficult to observe in the field. The moist color was indistinguishable from the dark-colored Bt horizon above (10YR 2/1). The only distinction made in the field was a reduction in clay estimation by feel (the buried A horizon had a silt loam texture, while Bt horizons above and below had silty clay textures).

One major limitation of this study was the inability to perform bulk density analysis by the same methodology across all sampling sites, due to the need to use different sampling equipment at sampling sites that were too wet to access with the truck-mounted Giddings probe. Comparison of bulk densities obtained by the clod method (used for the larger Giddings-probe cores) versus the core segment bulk densities (used for the smaller Geoprobe or AMS cores) do show some differences. Generally, the bulk densities of the subsoils were higher when the core segment method was used instead of the clod method. This can be expected to lead to overestimates of carbon and nitrogen stocks from the basins floors, which were least accessible with the truck-mounted Giddings probe. However, we found that this part of the basins generally had the lowest carbon and nitrogen stocks. Thus, the difference in bulk density methodology is unlikely to have produce this trend. To the contrary, the trend of lower carbon and nitrogen stocks in the basins may be stronger than reflected in the data collected in this study, as the difference in bulk density methods likely served to counteract this trend.

Conclusions

Compared to other depressional wetlands of the Great Plains and Central Lowlands, the Todd Valley deflation basins, like the Rainwater Basins, have relatively low levels of carbon and nitrogen. The basins are shown to have similar or lower carbon stocks than the uplands, except in one of the basins that contained a well-developed buried soils. This pattern is likely related to leaching losses of dissolved organic matter because overall carbon and nitrogen stocks are lowest in the soils with the best morphological evidence for leaching. Different types of wetlands can have remarkably different effects on carbon storage in the landscape, with sequestration rates reported in the literature ranging from 2 to 306 g C m^{-2} yr^{-1} (Mitsch et al., 2013). Here we demonstrate that deflation basin wetlands, even in relatively high rainfall areas, store much less carbon that other depressional wetlands of the Great Plains and Central Lowlands.

CHAPTER 4. GENERAL CONCLUSIONS

Morphological features present in the sampled soils included both albic and argillic horizons, redoximorphic features, and diffuse carbonates. Albic horizons were most common along basin edges, which were deeper and thicker than what is commonly observed in playa wetlands in the region. In the soil profiles from along the basin edge in Basins 1 and 3, there was evidence of deposition of colluvium over an older soil. One of the basins evaluated in this study was morphologically distinct from the other two, in that it contained finely disseminated carbonates and had no soils with albic horizons.

Todd Valley playa wetlands have relatively low levels of soil organic matter as compared to other wetlands. In one of the playas examined, soils from the basin edge had lower carbon and nitrogen compared to the uplands. This pattern is likely related to loss of dissolved organic matter due to leaching. In Basins 1 and 2, total carbon and nitrogen stock values showed no statistical difference ($p > 0.05$) between the upland, basin edge, and basin floor soils. In Basin 3, total carbon and nitrogen stock values showed a statistical difference ($p < 0.05$) between the upland, basin edge, and basin floor. A presumed buried soil in Basin 3 contains a high carbon percentage, which is attributed to slow decomposition due to anaerobic conditions. In the Great Plains region, playa wetlands store less carbon than other depressional wetlands.

The soils of the Todd Valley wetlands evince intense leaching, which is reflected in their morphology (e.g., development of albic horizons) and limits carbon and nitrogen storage. They also show evidence of infilling. Colluvial sediments infilling the basins results in an overthickened A horizon which may be difficult to distinguish form the underlying loess sediments. However, these sediments have undergone less eluviation and are therefore distinguished by a darker color and higher clay content.

Literature Cited

Airori, A. J., Baker, T. J., & Turk, J. K. (In Press). The Impact of Sampling Methodology on Soil Bulk Density Measurement by the Clod Method. *Communications in Soil Science and Plant Analysis*.

Amundson, R., Berhe, A. A., Hopmans, J. W., Olson, C., Sztein, A. E., & Sparks, D. L. (2015). Soil and human security in the 21st century. *Science, 348*(6235), 6. doi:10.1126/science.1261071

Assmus, R. J. (1993). *Genesis of the E horiozn in soils of the Massie Lagoon in Clay County, Nebraska.* (Ph.D.). University of Nebraska, Lincoln.

Bellamy, P. H., Loveland, P. J., Bradley, R. I., Lark, R. M., & Kirk, G. J. D. (2005). Carbon losses from all soils across England and Wales 1978-2003. *Nature, 437*(7056), 245-248. doi:10.1038/nature04038

Berhe, A. A., Harte, J., Harden, J. W., & Torn, M. S. (2007). The Significance of the Erosion-induced Terrestrial Carbon Sink. *BioScience, 57*(4), 337-346. doi:10.1641/b570408

Bettis, E., Muhs, D., Roberts, H., & Wintle, A. (2003). Last Glacial loess in the conterminous USA. *Quaternary Science Reviews*, 22(18-19), 1907-1946.

Birkeland, P.W. (1999). *Soils and Geomorphology (3rd Edition)*. New York: Oxford University Press, Inc.

Boone, R., Grigal, D., Sollins, P., Ahrens, R., & Armstrong, D. (1999). Soil sampling, preparation, archiving, and quality control. In G. Robertson, D. Coleman, C. Bledsoe, & P. Sollins (Eds.), *Standard soil methods for long-term ecological research*. New York: Oxford University Press.

Bowen, M. and W. Johnson. 2012. Late Quaternary environmental reconstructions of playa-lunette system evolution on the central High Plains of Kansas, United States. Geological Society of America Bulletin 124: 146-161. doi:10.1130/B30382.1.

Bowen, M. and W. Johnson. 2015. Holocene records of environmental change in High Plains playa wetlands, Kansas, US. Holocene 25: 1838-1851. doi:10.1177/0959683615591356.

Bowen, M.W. and W.C. Johnson. 2017. Anthropogenically accelerated sediment accumulation within playa wetlands as a result of land cover change on the High Plains of the central United States. Geomorphology 294: 135-145. doi:10.1016/j.geomorph.2017.02.017.

Bowen, M. W., Johnson, W. C., Egbert, S. L., & Klopfenstein, S. T. (2010). A GIS-based Approach to Identify and Map Playa Wetlands on the High Plains, Kansas, USA. *Wetlands, 30*(4), 675-684. doi:10.1007/s13157-010-0077-z

Busacca, A. J. (1989). Long Quaternary Record in Eastern Washington, USA, Interpreted from Multiple Buried Paleosols in Loess. Geoderma, 45(2), 105-122.

Drohan, P. J., Thompson, J. A., Lindbo, D. L., Beaudette, D. E., & Dadio, S. D. (2020). Redefining the fragipan to improve field recognition and land use relevance. *Soil Science Society of America Journal*, 84(4), 1055-1066.

Eggleston, K. (2013). SC ACIS Version 2 Retrieved from http://scacis.rcc-acis.org/

Elder, J., Beesley, T., & McKinzie, W. (1965). *Soil Survey of Saunders County, Nebraska*. Washington: United States Department of Agriculture - Soil Conservation Service.

Gross, C. D., & Harrison, R. B. (2018). Quantifying and Comparing Soil Carbon Stocks: Underestimation with the Core Sampling Method. *Soil Science Society of America Journal, 82*(4), 949-959. doi:10.2136/sssaj2018.01.0015

Guo, L. B., & Gifford, R. M. (2002). Soil carbon stocks and land use change: a meta analysis. *Global Change Biology, 8*(4), 345-360. doi:10.1046/j.1354-1013.2002.00486.x

Hallberg, G. R., Wollenhaupt, N. C., & Miller, G. A. (1978). Century of Soil Development in Spoil Derived from Loess in Iowa. Soil Science Society of America Journal, 42(2), 339-343.

Hartley, P., Presley, D., Ransom, M., Hettiarachchi, G., & West, L. (2014). Vertisols and Vertic Properties of Soils of the Cherokee Prairies of Kansas. Soil Science Society of America Journal, 78(2), 556-566.

Hirmas, D. R., & Mandel, R. D. (2017). Soils of the great plains. In L. T. West, M. J. Singer, & A. E. Hartemink (Eds.), *The Soils of the USA* (pp. 131-163). Cham, Switzerland: Springer.

Jacobs, P.M. and J.A. Mason. 2004. Paleopedology of soils in thick Holocene loess, Nebraska, USA. *Revista Mexicana de Ciencias Geologicas, 21*(1), p. 54-70.

Jacobs, P.M. and J.A. Mason. 2007. Late Quaternary climate change, loess sedimentation, and soil profile development in the central Great Plains: A pedosedimentary model. GSA Bulletin 119: 462-475. doi:10.1130/B25868.1.

Jobbagy, E. G., & Jackson, R. B. (2000). The vertical distribution of soil organic carbon and its relation to climate and vegetation. *Ecological Applications, 10*(2), 423-436. doi:Doi 10.2307/2641104

Khormali, F., & Kehl, M. (2011). Micromorphology and development of loess-derived surface and buried soils along a precipitation gradient in Northern Iran. Quaternary International, 234, 109-123.

Kolodynska-Gawrysiak, R. and J. Poesen. 2017. Closed depressions in the European loess belt - Natural or anthropogenic origin? Geomorphology 288: 111-128. doi:10.1016/j.geomorph.2017.02.004.

Koop, A. N., Hirmas, D. R., Sullivan, P. L., & Mohammed, A. K. (2020). A generalizable index of soil development. Geoderma, 360, 113898. doi:https://doi.org/10.1016/j.geoderma.2019.113898

Kuzila, M.S. 1995. Identification of multiple loess units within modern soils of Clay County, Nebraska. Geoderma 65: 45-57. doi:10.1016/0016-7061(94)00030-e.

Kuzila, M. and D. Lewis. 1993. Properties and genesis of loessial soils across a south-central Nebraska basin. Soil Science Society of America Journal 57(1): 155-161.

LaGrange, T.G., R. Stutheit, M. Gilbert, D. Shurtliff, and P.M. Whited. 2011. Sedimentation of Nebraska's Playa Wetlands: A Review of Current Knowledge and Issues. Nebraska Game and Parks Commission, Lincoln. 62 pages.

Lal, R. (2008). Carbon sequestration. *Philosophical Transactions of the Royal Society B-Biological Sciences, 363*(1492), 815-830. doi:10.1098/rstb.2007.2185

Mason, J. A. (2001). Transport direction of Peoria Loess in Nebraska and implications for loess sources on the central Great Plains. *Quaternary Research*, 56(1), 79-86.

Mason, J.A., P.M. Jacobs, R.S.B. Greene, & W.D. Nettleton. 2003. Sedimentary aggregates in the Peoria Loess of Nebraska, USA. *Catena, 53*, p. 377-397. doi: 10.1016/S0341-8162(03)00073-0.

Mason, J.A. & M.S. Kuzila. 2000. Episodic Holocene loess deposition in central Nebraska. Quaternary International 67: 119-131

Mason, J.A. & E.A. Nater. 1994. Soil Morphology – Peoria Loess Grain Size Relationships, Southeastern Minnesota. *Soil Science Society of America Journal, 58*, p. 432-439.

Miao, X. D., Mason, J. A., Johnson, W. C., & Wang, H. (2007). High-resolution proxy record of Holocene climate from a loess section in Southwestern Nebraska, USA. *Palaeogeography Palaeoclimatology Palaeoecology*, 245(3-4), 368-381.

Mitsch, W., Bernal, B., Nahlik, A. M., Mander, Ü., Zhang, L., Anderson, C. J., . . . Brix, H. (2013). Wetlands, carbon, and climate change. *Landscape Ecology, 28*(4), 583-597. doi:10.1007/s10980-012-9758-8

Mitsch, W., & Gosselink, J. (2007). *Wetland, 4th edn.* Hoboken: Wiley.

Mohammed, A.K., Hirmas, D.R., Nemes, A., Giménez, D., 2020. Exogenous and endogenous controls on the development of soil structure. Geoderma 357, 113945.

National Cooperative Soil Survey. (2012, June). SCOTT SERIES OSD. Retrieved February 18, 2019, from https://soilseries.sc.egov.usda.gov/OSD_Docs/S/SCOTT.html

Nitzsche, K. N., Kaiser, M., Premke, K., Gessler, A., Ellerbrock, R. H., Hoffmann, C., … Kayler, Z. E. (2017). Organic matter distribution and retention along transects from hilltop to kettle hole within an agricultural landscape. *Biogeochemistry*, *136*(1), 47–70. doi: 10.1007/s10533-017-0380-3

O'Geen, A. T. (2017). Series Extent Explorer. Retrieved from casoilresource.lawr.ucdavis.edu/see/

Post, W. M., Emanuel, W. R., Zinke, P. J., & Stangenberger, A. G. (1982). Soil carbon pools and world life zones. *Nature, 298*(5870), 156-159. doi:10.1038/298156a0

Presley, D. R., Ransom, M. D., Kluitenberg, G. J., & Finnell, P. R. (2004). Effects of thirty years of irrigation on the genesis and morphology of two semiarid soils in Kansas. *Soil Science Society of America Journal*, 68(6), 1916-1926. doi:DOI 10.2136/sssaj2004.1916

Rabenhorst, M.C. & K.A. Pershing. 2017. A Synthesized Manganese Oxide for Easily Making Durable Manganese-Coated IRIS Tubes. *Soil Science Society of America Journal*, *81*(1), p. 233-239.

Rabenhorst, M.C. & J. Post. 2018. Manganese Oxides for Environmental Assessment. *Soil Science Society of America Journal*.

Ritchie, J. C., McCarty, G. W., Venteris, E. R., & Kaspar, T. C. (2007). Soil and soil organic carbon redistribution on the landscape. Geomorphology, 89(1-2), 163-171.

Schaetzl, R., & Thompson, M. (2015). Soils: Genesis and Geomorphology 2nd edition. New York: Cambridge University Press.

Schoeneberger, P. J., Wysocki, D. A., Benham, E. C., & Staff, S. S. (2012). *Field book for describing and sampling soils, Version 3.0*. Lincoln, NE: Natural Resources Conservation Service, National Soil Survey Center.

Soil Survey Staff. (2014a). *Kellogg Soil Survey Laboratory Methods Manual. Soil Survey Investigations Report No. 42, Version 5.0* (R. Burt & Soil Survey Staff Eds.). Lincoln: U.S. Department of Agriculture, Natural Resources Conservation Service.

Soil Survey Staff. (2014b). Keys to Soil Taxonomy, 12th ed. In. Washington: United States Department of Agriculture-Natural Resources Conservation Service.

Soil Survey Staff. (2019). Official Soil Series Descriptions (OSDs). Retrieved from https://www.nrcs.usda.gov/wps/portal/nrcs/detail/soils/scientists/?cid=nrcs142p2_053587

Stockmann, U., Adams, M. A., Crawford, J. W., Field, D. J., Henakaarchchi, N., Jenkins, M., . . . Zimmermann, M. (2013). The knowns, known unknowns and unknowns of sequestration of soil organic carbon. *Agriculture Ecosystems & Environment, 164*, 80-99. doi:10.1016/j.agee.2012.10.001

Streeter, M. T., & Schilling, K. E. (2015). A comparison of soil properties observed in farmed, restored and natural closed depressions on the Des Moines Lobe of Iowa. *CATENA, 129*, 39-45. doi:10.1016/j.catena.2015.02.021

Stutheit, R.G., Gilbert, M.C., Whited, P.M., and Lawrence, K.L. (Eds.). (2004). *A Regional Guidebook for Applying the Hydrogeomorphic Approach to Assessing Wetland Functions of Rainwater Basin Depressional Wetlands in Nebraska* U.S. Army Engineer Research and Development Center.

Tiner, R.W. 2003. Geographically isolated wetlands of the United States. Wetlands 23(3): 494-516. doi:10.1672/0277-5212(2003)023[0494:giwotu]2.0.co;2.

Turk, J., Chadwick, O., & Graham, R. (2011). Pedogenic Processes. In P. Huang, Y. Li, & M. Sumner (Eds.), *Handbook of Soil Sciences: Properties and Processes, Second Edition* (pp. 30.31-30.29). Boca Raton: CRC Process.

Turk, J. K., & Graham, R. C. (2009). Soil Carbon and Nitrogen Accumulation in a Forested Debris Flow Chronosequence, California. *Soil Science Society of America Journal, 73*(5), 1504-1509. doi:10.2136/sssaj2008.0106

Turk, J., Young, R., Jelinski, N., Anderson, A., Dere, A., Moorberg, C., & Owen, R. (In Review). Soils of the central Nebraska Loess Hills and Central Loess Plains. *Great Plains Research.*

Turk, J.K., Goforth, B.R., Graham, R.C., Kendrick, K.J., 2008. Soil morphology of a debris flow chronosequence in a coniferous forest, southern California, USA. Geoderma 146 (1-2), 157–165.

United States Department of Agriculture, Natural Resources Conservation Service. 2006. *Land Resource Regions and Major Land Resource Areas of the United States, the Caribbean, and the Pacific Basin*. U.S. Department of Agriculture Handbook 296.

United States Department of Agriculture, Natural Resources Conservation Service. 2018. *Field Indicators of Hydric Soils in the United States,*Version 8.2. L.M. Vasilas, G.W. Hurt, and J.F. Berkowitz (eds.). USDA, NRCS, in cooperation with the National Technical Committee for Hydric Soils.

Veenstra, J. J., & Burras, C. L. (2015). Soil Profile Transformation after 50 Years of Agricultural Land Use. *Soil Science Society of America Journal, 79*(4), 1154-1162. doi:10.2136/sssaj2015.01.0027

Vepraskas, M.J., (2001). Morphological Features of Seasonally Reduced Soils. In J.L. Richardson & M.J. Vepraskas (Eds.), *Wetland Soils: Genesis, Hydrology, Landscapes, and Classification* (163-182). United States of America: Lewis Publishers.

Vepraskas, M.J. & S.P. Faulkner, (2001). Redox Chemistry of Hydric Soils. In J.L. Richardson & M.J. Vepraskas (Eds.), *Wetland Soils: Genesis, Hydrology, Landscapes, and Classification* (85-106). United States of America: Lewis Publishers.

Waring, B. G., Sulman, B. N., Reed, S., Smith, A. P., Averill, C., Creamer, C. A., . . . Schulz, M. (2020). From pools to flow: The PROMISE framework for new insights on soil carbon cycling in a changing world. *Global Change Biology, 26*(12), 6631-6643. doi:10.1111/gcb.15365

Basin 1, Transect 1.1											
Horizon	Depth (cm)	Boundary	Moist Color	Texture	Structure	Moist Consistence	Redox Conc.	Redox Depl.	Argillans	Effervesce	Roots
A1	0-23	C	10YR 2/2	SiC	GR, M, 2 to SBK, VF, 2	FRI		None	-	None	VF, 3
A2	23-45	G	10YR 2/1	SiCL	SBK, M, 2	VFR			-		VF, 3
Bt1	45-84	G	10YR 2/2	SiC	SBK, CO, 2	VFR			OAF		VF, 2
Bt2	84-106	C	10YR 2/2	SiC	SBK, M, 2	VFR			OAF		VF, 2
Bt3	106-139	G	10YR 3/3	SiC	PR, M, 2	FRI			CLF		VF, 1
Bt4	139-181	G	10YR 3/3 or 4/3	SiC	PR, M, 3	FIR			CLF		VF, 1
Bt5	181-218	C	10YR 4/3	SiC	PR, M, 2	FRI	Fe-Mn		CLF		VF, 1
BC	218-230+	-	10YR 4/4	SiC	SBK, M, 2	FRI	Fe-Mn		-		VF, 1
Basin 1, Transect 1.2											
Horizon	Depth (cm)	Boundary	Moist Color	Texture	Structure	Moist Consistence	Redox Conc.	Redox Depl.	Argillans	Effervesce	Roots
A1	0-38	C	10YR 2/1	SiCL	SBK, F, 2	FIR	Fe-Mn		-	None	3 VF
A2	38-52	C	10YR 3/1	SiCL	SBK, F, 2	FRI	-		-		3 VF
E	52-70	G	10YR 4/1	SiCL	ABK, M, 2	VFR	-		-		2 VF
Btss	70-120	A	10YR 2/1	SiCL	PR, M, 2	FRI	Fe-Mn		CLF w/ SS		2 VF
Bt	120-146	A	10YR 3/2	SiCL	ABK, M, 3	FRI	Fe-Mn		CLF		1 VF
Bt	146-166	G	10YR 4/2	SiCL	PL, VK, 2	FRI	Fe-Mn	Mn	CLF		1 VF
C1	166-188	C	10YR 4/2	SiCL	PL, TK, 2	FRI	Fe-Mn	Mn	-		1 VF
C2	188-200+	-	10YR 4/2	SiCL	PL, TK, 3	FIR	Fe-Mn	Mn	-		1 VF
Basin 1, Transect 1.3											
Horizon	Depth (cm)	Boundary	Moist Color	Texture	Structure	Moist Consistence	Redox Conc.	Redox Depl.	Argillans	Effervesce	Roots
Ap	0-18	C	10YR 2/1	SiCL	GR, F, 2	VFR	10	10	-	-	3, CO
E	18-53	C	10YR 2/1	SiL	SBK, F, 1	VFR	20	20	-		2, F
Bw	53-73	A	10YR 3/1	SiCL	PL, TN, 1	LO	-	-	-		1, VF
Bt1	73-123	A	10YR 2/1	C	PR, F, 1	FIR	-	-	CLF		3, F
Bt2	123-166	G	10YR 2/1	C	SBK, F, 2	FRI	-	-	CLF		1, VF
BC	166-186	G	10YR 3/2	C	PR, VF, 1	VFR	50	50	-		<1, VF
C	186-198+	-	10YR 4/3	SiC	MASS	FRI	>50	>50	-		-

Basin 1, Transect 2.1											
Horizon	Depth (cm)	Boundary	Moist Color	Texture	Structure	Moist Consistence	Redox Conc.	Redox Depl.	Argillans	Effervesce	Roots
Ap	0-26	C	10 YR 2/1	CL	3,M,GR	FRI	-			-	3, VF
A	26-55	A	10 YR 2/1	SiCL	2,M,SBK	VFR	-			-	2, VF
Bt1	55-87	G	10 YR 2/2	SiCL	2,M,PR	VFR	-		CLF	-	2, VF
Bt2	87-166	C	10 YR 2/2	SiCL	2,M,PR	VFR	Mn		CLF	-	1, VF
Bt3	166-194	G	10 YR 3/3	SiCL	2,M,PR	FRI	Mn		CLF	-	1, VF
Bt4	194-220	C	10 YR 3/4	CL	2,M,PR	FIRM	Mn		CLF	-	0
Bt5	220-241+	-	10 YR 3/4	SiCL	2,CO,SBK	FRI	Fe-Mn		CLF	-	0
Basin 1, Transect 2.2											
Horizon	Depth (cm)	Boundary	Moist Color	Texture	Structure	Moist Consistence	Redox Conc.	Redox Depl.	Argillans	Effervesce	Roots
A1	7-Jan	C	10YR 3/1	SiCL	3, GR, F	FR	N	N	-	-	3, VF
A2	22-Jul	A	10YR 2/1	SiC	2, SBK, VF	FR	N	N	-	-	3, VF
A3	22-48	G	10YR 2/1	SiC	2, SBK, M	FR	N	N	-	-	3, VF
E	48-64	C	10YR 4/1	SiC	2, SBK, M	FR	N	N	-	-	2, VF
Bt1	64-92	C	10YR 2/1	SiC	1, PR, M	FI	N	N	CLF	-	2, VF
Bt2	92-121	A	10YR 2/1	SiC	2, PR, M	FI	Y	N	CLF	-	2, VF
Bt3	121-144	C	10YR 3/2	SiC	1, PR, M	VF	Y	Y	CLF	-	2, VF
Bt4	144-158+	-	10YR 3/2	SiC	3, SBK, M	VF	Y	Y	CLF	-	1, VF
Basin 1, Transect 2.3											
Horizon	Depth (cm)	Boundary	Moist Color	Texture	Structure	Moist Consistence	Redox Conc.	Redox Depl.	Argillans	Effervesce	Roots
A1	0-15	C	10YR 2/1	SiL	SBK, M, 2	VFR	10	10	-	-	F, 2
A2	15-30	C	10YR 2/1	SiL	SBK, M, 2	FIR	10	10	-		F, 2
E	30-45	A	7.5YR 3/1	SiL	PL, VF, 1	VFR	20	20	-		F, 2
Bw1	45-64	D	10YR 3/2	SiCL	PL, VF, 1	LO	30	30	-		-
Bw2	64-136	A	10YR 3/2	C	PR, M, 2	FRI	30	30	-		F, 1
Bt	136-147	C	10YR 4/2	SiC	PR, F, 1	FIR	40	40	CLF		VF, 1
BC	147-178	C	10YR 4/3	C	SBK. M, 1	VFR	50	50	-		VF, 1
C	178-195+	-	10YR 4/4	C	MASS	VFR	50	50	-		-

Basin 1, Transect 3.1											
Horizon	Depth (cm)	Boundary	Moist Color	Texture	Structure	Moist Consistence	Redox Conc.	Redox Depl.	Argillans	Effervesce	Roots
A	0-22.5	A	10YR 2/1	Sicl	3C GR	FR	0	0	-	-	3 vf
Bt1	22.5-40.5	G	10YR 2/1	SiL	2M SBK	FR	0	0	CLF	-	3 vf
Bt2	40.5-64	C	10YR 2/1	SiL	3F PR	FR	0	0	CLF	-	3vf
Bt3	64-103.5	C	10YR 2/1	Sicl	2M SBK	FR	0	0	CLF	-	2 vf
Bt4	103.5-	-	10YR 3/1	Sicl	1F SBK	FI	0	0	CLF?	-	1 vf
Basin 1, Transect 3.2											
Horizon	Depth (cm)	Boundary	Moist Color	Texture	Structure	Moist Consistence	Redox Conc.	Redox Depl.	Argillans	Effervesce	Roots
A1	0-18	C	10YR 2/2		SBK, F, 2	FRI	Fe-Mn	-	-	None	VF, 3
A2	18-38	C	10YR 2/1		SBK, F, 1	FRI	Fe-Mn	-	-		VF, 2
E	38-60	A	10YR 3/1		PL, TK, 2	VFR	Fe-Mn	-	-		VF, 1
Bt1	60-102	G	10YR 2/1.5		ABK, M, 2	FIR	Fe-Mn	-	CLF		VF, 1
Bt2	102-129	C	10YR 2/1		PR, M, 2	FRI	Fe-Mn	-	CLF		VF, <1
Bt3	129-143	A	2.5Y 2.5/1		PL, M, 1	FRI	Fe-Mn	-	CLF		-
Bt4	143-171+	-	2.5Y 3/1		PL, TK, 2	FRI	Fe-Mn	Fe-Mn	CLF		-
Basin 1, Transect 3.3											
Horizon	Depth (cm)	Boundary	Moist Color	Texture	Structure	Moist Consistence	Redox Conc.	Redox Depl.	Argillans	Effervesce	Roots
A1	0-24	C	10YR 2/1	SiCL	SBK, M, 2	VFR	5	5	-		F, 3
A2	24-37	A	10YR 3/1	SiCL	SBK, M, 2	VFR	10	10	-		VF, 3
E	37-61	D	2.5Y 4/1	SiL	PL, TN, 1	VFR	20	20	-		-
Bw	61-85	C	10YR 3/2	SiC	PL, TN, 1	VFR	30	30	-		VF, <1
Bt1	85-103	C	10YR 3/2	C	PR, M, 2	FIR	40	40	CLF		VF, <1
Bt2	103-116	C	10YR 3/2	C	PR, M, 1	FRI	40	40	CLF		VF, <1
BC	116-148	A	10YR 4/3	C	PR, M, 1	FRI	50	50	-		VF, <1
C	148-218+	-	10YR 4/3	C	MASS	FRI	50	50	-		-

Basin 2, Transect 1.1											
Horizon	Depth (cm	Boundary	Moist Color	Texture	Structure	Moist Consistence	Redox Conc.	Redox Depl.	Argillans	Effervesce	Roots
A1	0-19	C	10YR 2/2	SICL	GR, 3, M	FRI			-		
A2	19-41	C	10YR 2/2	SICL	SBK, F, 2	VFR			-		
B	41-66	C	10YR 3/3	SICL	PR, M, 1	VFR			-		
Bt1	66-92	G	10YR 3/4	SICL	PR, M, 2	VFR			CLF		
Bt2	92-135	G	10YR 4/4	SICL	PR, M, 2	FRI			CLF		
Bt3	135-166	G	10YR 4/3	SICL	PR, M, 2	VFR			CLF		
C1	166-195	A	10YR 4/3	SICL	ABK, M, 1	FRI	Fe-Mn		-		
C2	195-228+	-	10YR 4/4	SICL	PL, TK, 2	VFR	Fe-Mn	Mn	-		
Basin 2, Transect 1.2											
Horizon	Depth (cm	Boundary	Moist Color	Texture	Structure	Moist Consistence	Redox Conc.	Redox Depl.	Argillans	Effervesce	Roots
A1	0-15	G	10YR 2/1.5		PL, TK, 2	FRI	Fe-Mn				VF, 3
A2	15-35	C	10YR 2/1		PL, TK, 1	VFR	Fe-Mn				VF, 3
AB	35-59	G	10YR 2/1		SBK, M, 1	VFR					VF, 3
Bt1	59-99	C	10YR 2/2		SBK, M, 1	VFR			CLF		VF, 2
Bt2	99-127	A	10YR 2/2		PR, M, 1	FRI			CLF		VF, 2
Bt3	127-159	C	10YR 3/2		PR, M, 1	FIR			CLF		VF, 1
Ct	159-208+	-	10YR 3/4		PR, F, 1.5	FIR		Fe-Mn	CLF		-
Basin 2, Transect 1.3											
Horizon	Depth (cm	Boundary	Moist Color	Texture	Structure	Moist Consistence	Redox Conc.	Redox Depl.	Argillans	Effervesce	Roots
Ap	0-17	G	2.5YR 2.5/1	SiL	SBK, M, 2	FRI	10	10	-	-	F, 3
A	17-31	C	5YR 2/1	SiL	SBK, M, 2	VFR	20	20	-	-	VF, 2
E	31-43.5	G	2.5Y 2.5/1	SiL	SBK, F, 2	VFR	~10	20	-	SLIGHT EFF	VF, 2
Bk	43.5-57	G	10YR 2/1	SiCL	SBK, M, 1	VFR	30	20	-	SLIGHT EFF	VF, 2
Btk	57-76.5	C	10YR 2/1	SiCL	SBK, M, 1	FIR	30	30	CLF	SLIGHT EFF	VF, 1
Bt1	76.5-110	A	10YR 2/2	SiCL	PR, M, 1	VFI	40	40	CLF	-	VF, 1
Bt2	110-118.5	G	5Y 2.5/1	SiCL	GR, M, 1	VFI	20	20	CLF	-	F, 2
Bt3	118.5-136	C	5Y 2.5/1	SiCL	GR, F, 1	FRI	40	40	OAF	-	VF, 1
BC	136-183	A	10YR 3/3	SiCL	GR, F, 1	FRI	>50	>50	-	-	VF, 1
C	183-222.5+	-	2.5Y 2.5/1	SiCL	MASS	FIR	>50	>50	-	-	VF, 1

Basin 2, Transect 2.1											
Horizon	Depth (cm	Boundary	Moist Color	Texture	Structure	Moist Consistence	Redox Conc.	Redox Depl.	Argillans	Effervesce	Roots
Ap1	0-9	C	10YR 2/2		GR, CO, 2	FRI	-	-	-		VF, 3
Ap2	9-19cm	C	10YR 2/2		GR, F, 2	VFR	-	-	-		VF, 3
Ap3	19-38	G	10YR 2/2		GR, F, 2	VFR	-	-	-		VF, 2
Bt1	38-64	C	10YR 3/3		SBK, M, 2	FRI	Mn	-	CLF		VF, 1
Bt2	64-93	G	10YR 3/3		SBK, M, 2	FRI	Fe-Mn	-	CLF		VF, 1
	93-127	C	10YR 3/4		SBK, M, 2	VFR	Fe-Mn	Fe-Mn	CLF		-
	127-153	C	10YR 4/4		PR, M, 2	FRI	Fe-Mn	Fe-Mn	CLF		-
	153-229+	-	10YR 4/4		PR, M, 2	FRI	Fe-Mn	Fe-Mn	-		-
Basin 2, Transect 2.2											
Horizon	Depth (cm	Boundary	Moist Color	Texture	Structure	Moist Consistence	Redox Conc.	Redox Depl.	Argillans	Effervesce	Roots
A	0-22	C	10YR 2/1	sicl	GR, F, 3	VFR	-	-	-		F, 3
A	22-55	A	10YR 2/1	sicl	SBK, M, 1	VFR	-	-	-		VF, 3
Bt	55-92	G	10YR 2/2	sil	SBK, M, 2	FRI	Mn	-	CLF		VF, 2
Btss	92-150+	-	10YR 4/3	sic	PL, TK, 2	FRI	Fe-Mn	-	CLFss		VF, 1
Basin 2, Transect 2.3											
Horizon	Depth (cm	Boundary	Moist Colc	Texture	Structure	Moist Consistence	Redox Conc.	Redox Depl.	Argillans	Effervesce	Roots
Ap1	0-26.5	G	10YR 2/1	SiL	GR, M, 1	VFR	30	30			3, F
Ap2	26.5-46	A	2.5YR 2/1	SiCL	GR, M, 1	VFR	30	30			1, VF
AB	46-61	C	5YR 2.5/1	SiCL	ABK, M, 2	FIR	30	30			1, VF
Bt1	61-134	A	10YR 2/1	SiC	ABK, F->M, 2	FIR	40	40	OAF		1, VF
Bt2	134-173	D	10YR 2/1	SiC	GR, M, 1	FRI	50	50	OAF		1, F
BC	173-196	A	7.5YR 3/2	SiL	ABK, F, 1	VFI	50	50			1, F
C	196-259	-	5Y 3/2	SiL	GR, F, 1	-	>50	>50			1, F

Basin 2, Transect 3.1											
Horizon	Depth (cm	Boundary	Moist Color	Texture	Structure	Moist Consistence	Redox Conc.	Redox Depl.	Argillans	Effervesce	Roots
A	0-14	C	10YR 4/2		SBK, VF, 2	FIR	-	-	-		VF, 3
A	14-46	C	10YR 3/2		SBK, F, 2	FRI	-	-	OAF		VF, 2
A	46-68	A	10YR 3/3		PR, M, 2	FRI	-	-	OAF		VF, 2
A	68-93	A	10YR 4/4		PR, M, 2	VFR	Mn	-	OAF		VF, 1
B	93-119	C	2.5Y 5/4		PL, M, 1	VFR	Fe-Mn 40%	Fe-Mn 40%	-		VF, 1
B	119-138	C	2.5Y 4/4		PL, M, 1	FIR	Fe-Mn 40%	Fe-Mn 40%	-		VF, 1
C	138-187	C	2.5Y 5/4		PL, TN, 1	VFR	Fe-Mn 50%	Fe-Mn 50%	-		VF, 1
C	187-232+	-	2.5Y 5/4		PL, TK, 1	VFR	Fe-Mn >50%	Fe-Mn >50%	-		VF, 1
Basin 2, Transect 3.2											
Horizon	Depth (cm	Boundary	Moist Colc	Texture	Structure	Moist Consistence	Redox Conc.	Redox Depl.	Argillans	Effervesce	Roots
Ap	0-4.5	C	10YR 2/2	SiCL	GR, F, 2	VFR	3%	3			F, 2
BA	4.5-28	G	10YR 2/2	SiC	SBK, 1, F	FRI	5%	5			F -> VF, 2
Bk1	28-49	C	10YR 4/3	SiC	PL, TK, 2->1	FIR	15%	15		VIOLENT	VF, 1
Bk2	49-90	C	10YR 5/3	SiC	PL, TK, 1	VFR	30%	30	CLF	VIOLENT	VF, 1
Bk3	90-113.5	C	10YR 5/3	C	PL, TH, 2	VFR	50%	50		MOD	VF, 1
Bk4	113.5-138	A	10YR 5/3	SiC	PL, TH, 1	VFR	50%	50		MOD -> SLIGHT	VF, <1
BC	138-168	C	10YR 5/3	C	SBK, CO, 2	VFR	60%	60		SLIGHT	
C1	168-214	C	2.5Y 5/3	SiCL	SBK, M, 2	VFR	60%	60		SLIGHT	
C2	214-246	G	2.5Y 5/3	SiCL	MASS	VFR	60%	60		V SLIGHT	
C3	246-277+	-	10YR 5/3	SiCL	MASS	VFR	60%	60		V SLIGHT	
Basin 2, Transect 3.3											
Horizon	Depth (cm	Boundary	Moist Color	Texture	Structure	Moist Consistence	Redox Conc.	Redox Depl.	Argillans	Effervesce	Roots
A1	0-14	A	5YR 2/1	SiL	GR, 1, F	VFR	20	20	-		F, 3
A2	14-22	C	5YR 2/1	SiL	GR, 2, F	FRI	30	30	-		F, 3
A3	22-30	A	10YR 2/1	SiL	SBK, 1, F	VFR	30	30	-		F, 2
E	30-48	G	5YR 2.5/2	SiL	PL, 1, M	VFR	10	10	-		F, 2
Bt1	48-118	A	10YR 2/1	SiC	PR, 2, F	FIR	-	-	CLF		VF, 2
Bt2	118-146	C	10YR 2/1	SiCL	SBK, 1, M	FRI	-	-	CLF		VF, 1
BC	146-212	C	7.5YR 3/1	SiCL	PR, 2, F	FIR	40	40	-		VF, 1
C	212-230+	-	10YR 3/2	SiCL	MASS	FRI	>50	>50	-		-

Basin 3, Transect 1.1											
Horizon	Depth (cm)	Boundary	Moist Color	Texture	Structure	Moist Consistence	Redox Conc.	Redox Depl.	Argillans	Effervesce	Roots
A1	0-11	C	10YR 2/2	SiCL	SBK, M, 3	FIR	-	-	-	None	VF, 3
A2	11-28cm	C	10YR 2/1	SiCL	PL, M, 2	FRI	-	-	-		VF, 3
A3	28-47	G	10YR 2/1	SiCL	PL, VK, 2	VFR	-	-	-		VF, 2
A4	47-76	A	2.5Y 3/1	SiClL	SBK, M, 2	VFR	-	-	-		VF, 2
Bt1	76-121	C	10YR 3/1	C	PR, M, 2	FIR	-	-	CLF		VF, 1
Bt2	121-168	A	10YR 3/1	C	SBK, F, 3	FRI	Fe-Mn 10%	Fe-Mn 10%	CLF		VF, <1
Bt3	168-195	G	10YR 3/1	SiC	PR, M, 1.5	FRI	Fe-Mn 30%	Fe-Mn 20%	CLF		-
C	195-220+	-	10YR 4/1	SiC	PL, TK, 1	FRI	Fe-Mn >50%	Fe-Mn 50%	-		-
Basin 3, Transect 1.2											
Horizon	Depth (cm)	Boundary	Moist Color	Texture	Structure	Moist Consistence	Redox Conc.	Redox Depl.	Argillans	Effervesce	Roots
A1	0-17	A	10YR 2/1	SiCL	SBK, F, 2	FIR	Fe-Mn 5%	Fe-Mn 5%	-	-	F, 3
A2	17-34	C	10YR 2/1	SiL	PL, M, 2	FRI	Fe-Mn	Fe-Mn	-	-	F, 2
E	34-63	A	10YR 3/1 to 4/1	SiL	PL, TN, 2	VFR	Fe-Mn	-	-	-	VF, 2
Bt1	63-90	G	2.5Y 3/1	SiC	PR, F, 3	FIR	Fe-Mn	Fe-Mn	CLF	-	VF, 2
Bt2	90-151	C	10YR 2/1	C	PR, F, 3	FIR	Fe-Mn	Fe-Mn	CLF	-	VF, 1
Bt3	151-186	C	10YR 2/1	SiC	SBK, M, 2	FIR	Fe-Mn	Fe-Mn	CLF	-	Few
Bt4	186-208+	-	10YR 3/1	SiC	SBK, M, 2	FRI	Fe-Mn	Fe-Mn	CLF	-	Few
Basin 3, Transect 1.3											
Horizon	Depth (cm)	Boundary	Moist Color	Texture	Structure	Moist Consistence	Redox Conc.	Redox Depl.	Argillans	Effervesce	Roots
Ap	0-10.5	C	N 2.5/-	SiL	-	VFR	10	10	-	-	-
A	10.5-23.5	C	N 2.25/-	SiL	-	VFR	20	20	-	-	-
E	23.5-35	A	2.5Y 2.5/1	SiL	-	VFR	20	20	-	-	-
Bt1	35-98	A	10YR 2/1	SiC	-	FIR	-	-	CLF	-	-
Bt2	98-142	C	10YR 2/1	SiC	-	FIR	-	-	CLF	-	-
Bt3	142-216	G	10YR 2/1	SiC	-	FIR	40	40	CLF	-	-
BC	216-248+	-	10YR 2/2	SiCL	-	FRI	40	40	-	-	-

Basin 3, Transect 2.1											
Horizon	Depth (cm)	Boundary	Moist Color	Texture	Structure	Moist Consistence	Redox Conc.	Redox Depl.	Argillans	Effervesce	Roots
Ap	0-14	C	10YR 2/1 or 2	SiCL	Mass.	FIR	-	-	-	-	VF, 3
A1	14-42	C	10YR 2/1	SiL	SBK, M, 3	FRI	-	-	-	-	VF, 3
A2	42-69	G	10YR 2/1	SiCL	SBK, F, 2	VFR	-	-	-	-	VF, 2
Bw	69-90	G	10YR 2/1	SiC	SBK, F, 2	FIR	-	-	-	-	VF, 1
Bt1	90-141	C	10YR 4/3	SiC	SBK, M, 1	FIR	Fe-Mn 10%	Fe-Mn 10%	CLF	-	VF, <1
Bt2	141-196	C	10YR 5/3	SiC	PR, M, 1	VFR	Fe-Mn 20%	Fe-Mn 30%	CLF	-	VF, <1
C1	196-222	A	10YR 4/3	SiC	Mass.	VFR	Fe-Mn 10%	Fe-Mn 20%	-	-	-
C2	222-233+	-	10YR 4/3	SiC	Mass.	VFR	Fe-Mn 10%	Fe-Mn 10%	-	-	-
Basin 3, Transect 2.2											
Horizon	Depth (cm)	Boundary	Moist Color	Texture	Structure	Moist Consistence	Redox Conc.	Redox Depl.	Argillans	Effervesce	Roots
Ap	0-8	C	10YR 2/1	SiCL	GR, M, 2	FRI	Fe-Mn		-	-	F, 3
A	8-23cm	C	10YR 2/1	SiCL	SBK, M, 2	VFI	Fe-Mn	Fe-Mn	-	-	F, 3
AB	23-34	A	10YR 2/1	SiCL	GR, F, 2	VFR	Fe-Mn	Fe-Mn	-	-	F, 2
Bw	34-50	G	2.5Y 2.5/1	SiL	SBK, M, 1	VFR	Fe-Mn	Fe-Mn	-	-	VF, 1
Bt1	50-69	A	2.5Y 3.5/1	SiL	PL, M, 2	VFR	Fe-Mn	Fe-Mn	CLF	-	-
Bt2	69-89	A	2.5Y 3/1	SiCL	SBK, M, 2	FRI	Fe-Mn	Fe-Mn	CLF	-	-
Bt3	89-155	C	10YR 2/2	C	SBK, M, 2	FIR	Fe-Mn	Fe-Mn	CLF	-	-
Bt4	155-176+	-	10YR 4/2	C	PL, TK, 3	VFR	Fe-Mn	Fe-Mn	CLF	-	-
Basin 3, Transect 2.3											
Horizon	Depth (cm)	Boundary	Moist Color	Texture	Structure	Moist Consistence	Redox Conc.	Redox Depl.	Argillans	Effervesce	Roots
A	0-22	D	10YR 2/1	SiL	GR, F, 1	VFR	5	5	-		F, 3
AE	22-40	C	10YR 2/1	SiL	PL, M, 2	VFR	5	5	-		F, 2
Bt	40-105	A	10YR 2/1	SiC	SBK, M, 1	FRI	10	10	CLF		F/VF, 3
E/Btb*	105-128	C	10YR 2/1	SiL	SBK, F, 1	FRI	10	10	CLF		VF, 3
Btb	128-160	C	10YR 2/1	SiC	SBK, M, 3	FIR	5	5	CLF		VF, 2
BCb	160-172	G	7.5YR 2.5/1	SiCL	MASS	FIR	50	50	-		VF, 1
Cb	172-206+	-	10YR 3/2	SiCL	MASS	FRI	60	60	-		VF, 1

Basin 3, Transect 3.1											
Horizon	Depth (cm)	Boundary	Moist Color	Texture	Structure	Moist Consistence	Redox Conc.	Redox Depl.	Argillans	Effervesce	Roots
Ap1	0-11	A	10YR 3/3	SiCL	SBK, F, 2	FIR					VF, 3
Ap2	11-37cm	G	2.5Y 4/3	C	GR, F, 1	FRI					VF, 3
A	37-55	A	10YR 2/1	SiCL	PL, TH, 2	VFR					VF, 2
AB1	55-72	C	10YR 2/1	SiCL	SBK, M, 2	FRI					VF, 2
AB2	72-105	A	10YR 3/1	SiCL	SBK, M, 2	FIR					VF, 2
Bt1	105-144	G	10YR 2/1	C	PR, M, 2	FIR	Fe-Mn	Fe-Mn	CLF		VF, 1
Bt2	144-171	C	10YR 3/1	C	PR, M, 2	FIR	Fe-Mn	Fe-Mn	CLF		DECOMP
Bt3	171-196	G	10YR 4/2	C	PR, M, 1	FIR	Fe-Mn	Fe-Mn	CLF		DECOMP
Bt4	196-220+	-	10YR 4/2	SiC	PR, M, 1	FIR	Fe-Mn	Fe-Mn	CLF		DECOMP
Basin 3, Transect 3.2											
Horizon	Depth (cm)	Boundary	Moist Color	Texture	Structure	Moist Consistence	Redox Conc.	Redox Depl.	Argillans	Effervesce	Roots
A1	0-18	C	10YR 2/1	SiCL	SBK, M, 2	VFI	<5, Fe-Mn	<5, Fe-Mn	-	-	F, 3
A2	18-34	A	10YR 2/1	SiCL	SBK, M, 2	VFR	<5, Fe-Mn	<5, Fe-Mn	-	-	VF, 3
A3	34-62	C	2.5Y 2.5/1	SiCL	PL, TN, 3	VFR	5, Fe-Mn	-	-	-	VF, 2
E	62-74	A	2.5Y 4/1	SiCL	PL, M, 1	FRI	<5, Fe-Mn	10, Fe-Mn	-	-	VF, 1
Bw	74-86	C	2.5Y 2.5/1	SiC	SBK, M, 1	VFI	15, Fe-Mn	15, Fe-Mn	-	-	VF, <1
Bt1	86-121	G	10YR 3/1	C	ABK, M, 2	VFI	15, Fe-Mn	15, Fe-Mn	CLF	-	VF, <1
Bt2	121-166	G	2.5Y 3/2	C	ABK, M, 1	VFI	15, Fe-Mn	15, Fe-Mn	CLF	-	-
Ct	166-210+	-	10YR 2/2	C	SBK, CO, 2	FRI	15, Fe-Mn	15, Fe-Mn	CLF	-	-
Basin 3, Transect 3.3											
Horizon	Depth (cm)	Boundary	Moist Color	Texture	Structure	Moist Consistence	Redox Conc.	Redox Depl.	Argillans	Effervesce	Roots
Ap	0-23.5	C	5YR 2/1	SiCL	GR, 2, M	VFR	10	10	-	-	F, 3
A	23.5-44	C	5Y 2/1	SiCL	SBK, 2, F	VFR	20	20	-	-	F, 3
E	44-60	A	5YR 2/1	SiCL	PL, 1, M	VFR	10	10	-	-	VF, 2
Bt1	60-116	A	5YR 2/1	SiCL	PL, 1, M	FRI	<10	<10	CLF	-	VF, 2
Bt2	116-173	C	10YR 2/1	SiC	SBK, 2, M	FRI	-	-	CLF	-	VF, 1
Bt3	173-189	G	2.5Y 2.5/1	SiC	SBK, 2, F	FRI	-	-	CLF	-	-
C	189-233+	-	10YR 2/1	SiL	PL, 1, M	VFR	30	30	-	-	-